Cleaner Materials 11 (2024) 100226

Contents lists available at ScienceDirect

Cleaner Materials

journal homepage: www.journals.elsevier.com/cleaner-materials

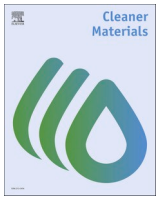

Experimental feasibility study of using eco- and user-friendly mechanochemically activated slag/fly ash geopolymer for soil stabilization

Mukhtar Hamid Abed [a,f,1,*], Firas Hamid Abed [a,b,7], Seyed Alireza Zareei [b,6], Israa Sabbar Abbas [c,d,2], Hanifi Canakci [e,3], Nahidh H. Kurdi [f,4], Alireza Emami [b,5]

[a] Projects Department, Al Ramadi Municipality, Anbar Province, Iraq
[b] Department of Civil Engineering, Khorasgan (Isfahan) Branch, Islamic Azad University, Isfahan, Iran
[c] Department of Civil Engineering, Al-Qalam University, Kirkuk, Iraq
[d] Department of Civil Engineering, Kirkuk University, Kirkuk, Iraq
[e] Department of Civil Engineering, Hasan Kalyoncu University, Gaziantep, Turkey
[f] Department of Civil Engineering, University of Anbar, Anbar, Iraq

ARTICLE INFO

Keywords:
Geopolymer
Mechanochemical activation
Soil stabilization
Durability properties
Sulfate attack

ABSTRACT

This study focuses on the development of eco and user-friendly mechanochemically-activated geopolymeric stabilizers, surpassing the limitations inherent in traditional geopolymerization methods. A comparative analysis was undertaken with conventionally activated geopolymer stabilizers to establish benchmarks for effectiveness in soil stabilization applications. Additionally, the research delves into the impact of granulated blast-furnace slag (GGBS) content on the mechanical and durability properties of stabilized soil samples. In addition, the investigation focuses on the influence of the activation method on soil effectiveness and strength post-exposure to sulfate attack. The durability performance is rigorously assessed through the immersion of specimens in a 1 % magnesium sulfate ($MgSO_4$) solution for 60 and 120 days. The comprehensive evaluation includes visual appearance, mass changes, Ultrasonic Pulse Velocity (UPV), Unconfined Compressive Strength (UCS), and Fourier-Transform Infrared (FTIR) spectra of geopolymer-stabilized soil specimens. The results showed that before the exposure to the $MgSO_4$ solution, the UCS of mechanochemically activated geopolymer (MAG) samples was higher (12–45 %) than that of conventionally activated geopolymer (CAG)-stabilized soil. Furthermore, the strength of the geopolymer-stabilized soil improved by 114 %, 247 %, and 361 %, at 50, 75, and 100 % GGBS content, respectively. On the other hand, after exposure to the $MgSO_4$ solution, the results showed that the mechanochemically activated geopolymer-stabilized soil has better resistance to sulfate erosion than the conventionally activated geopolymer-stabilized soil. The residual UCS for MAG and CAG samples were 93 % and 89 % when exposed to 1 % magnesium sulfate solution for 60 days, whereas they declined to 70 % and 58 %, respectively, after 120 days of immersion.

Introduction

In recent years, the deep soil mixing (DSM) technique has become more popular for stabilizing soft to very soft clays due to its speed and cost-effectiveness (Arulrajah et al., 2018). For earthworks exposed to a range of loads of low to medium, such as road embankments, the deep soil mixing approach is more feasible and cost-effective than alternatives, such as piling (Bouazza et al., 2004; Porbaha, 1998). Ordinary

* Corresponding author.
E-mail addresses: eng.mukhtar92@gmail.com (M. Hamid Abed), a.r.zareei@khuisf.ac.ir (S. Alireza Zareei), israasabbar52@gmail.com (I. Sabbar Abbas).
[1] 0000-0002-8940-8533.
[2] 0000-0003-4632-9146.
[3] 0000-0002-1392-1701.
[4] 0000-0003-1847-2965.
[5] 0000-0003-0377-2228.
[6] 0000-0002-4869-4174.
[7] 0000-0002-5159-3489.

https://doi.org/10.1016/j.clema.2024.100226
Received 10 September 2023; Received in revised form 1 January 2024; Accepted 11 February 2024
Available online 15 February 2024

Portland cement (OPC) is the traditional binder utilized with this approach, with binder levels of up to 30 % by soil mass (Shen et al., 2003; Horpibulsuk et al., 2011; Bruce et al., 2013). Environmental concerns are related to the use of cement due to the implied extensive use of natural resources and energy, in addition to the release of CO_2 during the production of these common binders. Therefore, recent studies are researching alternate binders that can reduce the carbon footprint of construction works (Arulrajah et al., 2018).

In recent years, there has been a growing interest in geopolymer materials as a feasible alternative to ordinary Portland cement (OPC) (Juenger et al., 2011). According to Nedunuri and Muhammad, (2020), geopolymerization is a process that occurs when an aluminosilicate precursor reacts with an alkaline activator, leading to the creation of a geopolymer that possesses an amorphous microstructure. Geopolymer materials offer several advantages over OPC, including their eco-friendliness, chemical resistance, durability, excellent mechanical characteristics, resistance to alkali-aggregate reactions, and the visco-plastic constitutive relationship like that of the OPC. These characteristics make geopolymer materials a promising alternative to OPC for various applications (Bilondi et al., 2018; Favier et al., 2014; Pacheco-Torgal et al., 2011; Pacheco-Torgal et al., 2008; Palacios et al., 2008; Çevik et al., 2018). Recently, several studies have explored the application of geopolymers as soil stabilizers (Rios et al., 2019; Sargent et al., 2016; Phummiphan et al., 2016; Yaghoubi et al., 2019; Cyriaque Kaze et al., 2022; Kaze et al., 2021). The geopolymer binder aids in the formation of a denser microstructure in soil particles, thereby improving volume stability and mechanical properties (Zhang et al., 2013). Consequently, geopolymers can be effectively utilized as shallow-depth soil stabilizers (e.g., for base or subbase in pavement, embankment, shallow foundation, airport construction, etc.) and in deep soil mixing applications (Phummiphan et al., 2016; Teerawattanasuk and Voottipruex, 2019).

Although the geopolymer binder has great potential as an environmentally friendly alternative to OPC, its use has been limited to moderate applications until recently. Encouraging the use of geopolymers in construction can greatly enhance their environmental friendliness. However, the conventional method of producing geopolymers involves a two-part process that utilizes alkaline solutions and solid alumina-silica precursors. According to Lee, (2002) and, Lee and Van Deventer, (2003), the hazardous activators are responsible for dissolving the raw materials and regulating the mechanical properties of the geopolymer. Although conventional geopolymer formulations have their advantages, their two-part mix formulations have some drawbacks, as indicated in (Duxson and Provis, 2008). Handling the alkali solution can be hazardous and pose a risk of accidents on-site. To facilitate the widespread commercialization of geopolymeric materials, it is essential to replace the conventional activation method, which is not user-friendly. The dissolution of NaOH in water is an exothermic process that produces a hazardous alkaline medium, presenting significant challenges for safety and handling. Thus, it is necessary to develop an alternate activation method that can overcome these limitations and enable the use of geopolymer materials in a solid form, similar to OPC. The use of solid-form geopolymers represents an innovative approach to mitigating the issues associated with conventional geopolymeric systems, and eliminates the need to handle highly alkaline solutions to activate geopolymers. By developing alternative approaches to activate geopolymers, it is possible to enhance their practicality and environmental sustainability, and enable their widespread use in the construction industry.

Mechanochemical activation is an innovative solid-state chemistry method for producing geopolymers. It involves the milling or grinding of small particulate solid matter to create molecularly dense, reactive, and amorphous aggregated composite particles. According to Hamid Abed et al., (2022a, 2022b), this process involves co-grinding solid binders, such as GGBS, fly ash, rice husk ash, and other aluminosilicate sources, with solid alkali activators, such as sodium hydroxide and sodium silicate, in a ball grinder. As a result, only water is needed to initiate the geopolymerization reaction process. The intense milling or grinding processes can generate surface defects and electrostatic charges, increasing surface energy and a phase change from crystalline to amorphous (Intini et al., 2009; Baláž et al., 2013) and activated particle agglomeration (Souri et al., 2015). A recent study indicates that the mechanochemical activation process can increase reactivity, alter the polymerized unit structure, and considerably improve the mechanical properties of hydrated products (Gupta et al., 2017; Mudgal et al., 2019; Matalkah et al., 2017; Kumar and Kumar, 2011). Hosseini et al., (2021) reported that the mechanochemical synthesis process increased the dispersion of fly ash -bottom ash particles, altered the alkali activators and aluminosilicate reaction kinetics, increased the interconnectivity of geopolymer structure, and declined pore size, resulting in an improvement in mechanical characteristics of 60 % to 80 %. Hamid Abed et al., (2022b, 2022c) found that the mechanochemical activation approach enhanced the UCS by (22–44 %) in comparison with conventionally activated geopolymer grout and was higher (41–73 %) than that of One-part geopolymer grout. Kushwah et al., (2021) developed a geopolymeric binder in solid form by mechanochemical synthesis of fly ash and dry alkaline activator after different hours of ball-milling. The results revealed that the influence of milling duration was substantial between 2 h and 6 h, and the strength performance was significantly increased; however, the strength decreased when the grinding length exceeded 6 h. (8, 10, and 12 h). Abbas et al., (2022) investigated the feasibility of incorporating rice husk ash as an incomplete antecedent in GGBS-based geopolymer grout which was mechanochemically activated. They found that the mechanochemically activated geopolymer grout with 20 % rice husk ash increased UCS by 28 % and 27 % compared to OPC and conventionally activated geopolymer grout, respectively.

The durability of stabilized soils is a crucial design consideration for deep soil mixing, particularly in harsh environments (chemical attacks, carbonation, Ca^{+}, freezing/thawing, and wetting/drying cycles) (Denies et al., 2015; Bellato et al., 2012; Ikegami et al., 2003). Sulfate attack is one of the most significant elements affecting the constructions' long-term endurance (Goncalves et al., 2019; Zhu et al., 2021). In practice, underground constructions may be subjected to sulfates when groundwater is contaminated (agricultural, industrial, or air pollution) or gypsum is present in the soil. Therefore, in DSM, water and sulfated soils may constitute the soil–cement material, thereby enhancing their negative influence. It is well known that the various types of sulfate assaults produce mechanical and chemical deterioration in clayey soils in particular (Helson et al., 2018). According to the authors, there may potentially be an interaction between clay and sulfate ions (Sherwood, 1962; Puppala et al., 2007). Verástegui-Flores and Di Emidio, (2014) indicate that external sulfate attacks can degrade clay-cement samples by lowering shear modulus and increasing hydraulic conductivity. The sort of binder utilized is the primary factor determining the degree of resistance to chemical attacks. Jiang et al., (2018) utilized a lightweight alkali-activated GGBS as a binder to stabilize fill soil in subgrade work and then immersed stabilized soil samples in a sulfate solution for various periods (3, 7, 14, 28, 60, 90, and 120 days). The results demonstrate that lightweight alkali-activated GGBS-stabilized soil has superior resistance to sulfate attack in terms of increased water absorption and improved mechanical properties; the increased cementitious hydration products can explain it in the stabilized soil.

The novelty of this study lies in the exploration of mechanochemically activated slag/fly Ash geopolymer stabilizers, which have not been previously investigated for the specified research objective. The primary focus is on developing environmentally and user-friendly mechanochemically activated geopolymeric stabilizers, addressing the limitations of traditional geopolymerization methods. A comparative analysis with conventionally activated geopolymer stabilizers is conducted to establish benchmarks for effectiveness in soil stabilization applications. Additionally, the research investigates the influence of GGBFS content on the mechanical and durability properties of stabilized soil samples.

Notably, little attention has been given to the long-term durability of geopolymer-stabilized soils, especially regarding the impact of the activation method on soil effectiveness and strength after exposure to sulfate attack. The durability performance is assessed by immersing specimens in a 1 % magnesium sulfate (MgSO4) solution for 60 and 120 days. The evaluation encompasses visual appearance, mass changes, Ultrasonic Pulse Velocity (UPV), Unconfined Compressive Strength (UCS), and Fourier-Transform Infrared (FTIR) spectra of geopolymer-stabilized soil specimens. This research aims to contribute to the advancement of geopolymer synthesis methods and provide valuable insights into the long-term durability of geopolymer-stabilized soils.

Materials and methods

Materials

The fine-grained soil was examined for deep mixing in the experimental investigation obtained from Gaziantep, Turkey, as shown in Fig. 1. In accordance with the Unified Soil Classification System (USCS), the soil is thought to be a low-plastic clay and classified as CL. The soil was dried in an oven for 24 h and sieved through a 0.425 mm sieve in accordance with the standardized method to prepare remoulded specimens for laboratory testing (IS: 2720- Part 1), and the soil characteristics used in this study are given in Table 1.

GGBS and class F fly ash were used as the raw precursors to produce geopolymer binder. A 2.5 M concentration of sodium hydroxide (NaOH) solution was prepared using 97–98 % pure NaOH beads bought locally. Sodium silicate (Na_2SiO_3) was adopted in two forms: a liquid solution for the preparation of traditional geopolymer and a powder form (metasilicate-Penta) for the production of mechanochemical geopolymer binder. In accordance with previously published research applying the mechanochemical synthesis method (Abbas et al., 2022; Bhardwaj et al., 2020; Gupta et al., 2017, 2020; Hamid Abed et al., 2022b; Mudgal et al., 2019; Manish et al., 2016), the ratio of Na_2SiO_3/NaOH = 0.5 was adopted to prepare the alkali activator. The chemical characteristics and the physical properties of GGBS, fly ash, Na_2SiO_3, and clay are all presented in Table 2.

Characterization of geopolymer binders

In this study, the preparation of mechanochemically activated geopolymer (MAG) stabilizers involved grinding all raw material powders (NaOH, metasilicate, slag, and fly ash) for 2 h as described by Hamid Abed et al., (2022b) (Fig. 2). The grinding process was conducted using a ball mill of 80 kg capacity using 12 balls, each with a mass of 400 g and a diameter of 45 mm. Through the ball milling process (grinding), the components (particles) of mixed raw materials are trapped between the balls and the container wall, which is caused by the continuous impact of the particles and grinding. After that, The resulting MAG powder (Fig. 2) was mixed with tap water to produce a MAG stabilizer, following the procedure outlined by Abbas et al., (2022) and, Hamid Abed et al., (2022b, 2022c).

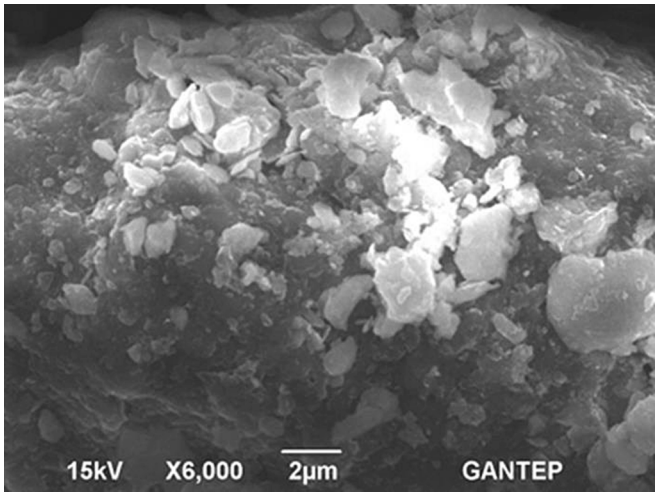

Fig. 1. SEM pictures clay soil.

Table 1
Characteristics of soil (clay).

Parameters	Value
Liquid limit (LL)	41
Plastic limit (PL)	25
Plasticity index (PI)	16
Specific gravity (Gs)	2.77
passing No.200	90
Optimum moisture content, OMC, (%)	19.2
Maximum dry unit weight (kN/m^3)	17.5
Swelling (%)	3.58
Silt (%)	32
Clay (%)	58
Classification (USCS)	CL

Table 2
Chemical characteristics and physical properties of FA, GGBS, sodium silicates and clay.

Constituent (%)	GGBS	FA	(Na_2SiO_3-Penta) Powder	(Na_2SiO_3) liquid	clay
a) Chemical composition					
CaO	34.19	4.24			18.24
Al_2O_3	10.6	24.4			6.36
SiO_2	40.42	57.2	28	29.4	17.25
Fe_2O_3	1.28	7.1			10.7
MgO	7.63	2.4			0.44
SO_3	0.68	0.29			0.08
K_2O	0.0128	3.37			1.49
Na_2O		0.38	29	14.7	
H_2O			43	59.9	
loss of ignition	1.64	2.07			
Modulus ratio			1	2	
b) Physical properties					
Specific surface (m^2/kg)	565	379			
Specific gravity	2.9	2.2			

The mechanochemically activated geopolymer slurry mixture, with a water-to-binder ratio of 1 (equivalent to 2.5 molarity), and soil (clay) at the optimal moisture content of LL-5 were mixed at a binder-to-soil ratio of 30 % to produce soil-binder (DSM) specimens. These specimens were cured for 28, 60, and 120 days in well-sealed plastic bags at 23 °C ± 3 before UCS testing.

To facilitate comparative analysis, a conventionally activated geopolymer slurry mixture is introduced as a substitute for the mechanochemically activated geopolymer slurry in the formulation of CAG-stabilized soil. This substitution allows for an exploration of the differential effects between the two activation methods on the soil stabilization process. hydroxide (NaOH) beads were dissolved in tap water at a molarity of 2.5, and the weight of the dissolved NaOH was measured for conventional geopolymer preparations It is worth mentioning that the mixing process resulted in an exothermic reaction, which led to the NaOH solution becoming excessively hot. Consequently, the liquid was allowed to cool to ambient temperature and stored until chemical equilibrium was achieved before further use. Subsequently, sodium silicate (Na_2SiO_3) was added to the cooled sodium hydroxide liquid as per the conventional geopolymer activation procedure. This cautious approach was adopted to ensure the safe handling of the highly alkaline NaOH solution and to minimize the risks associated with the exothermic reaction.

This study utilized two mixture groups (MAG and CAG), each

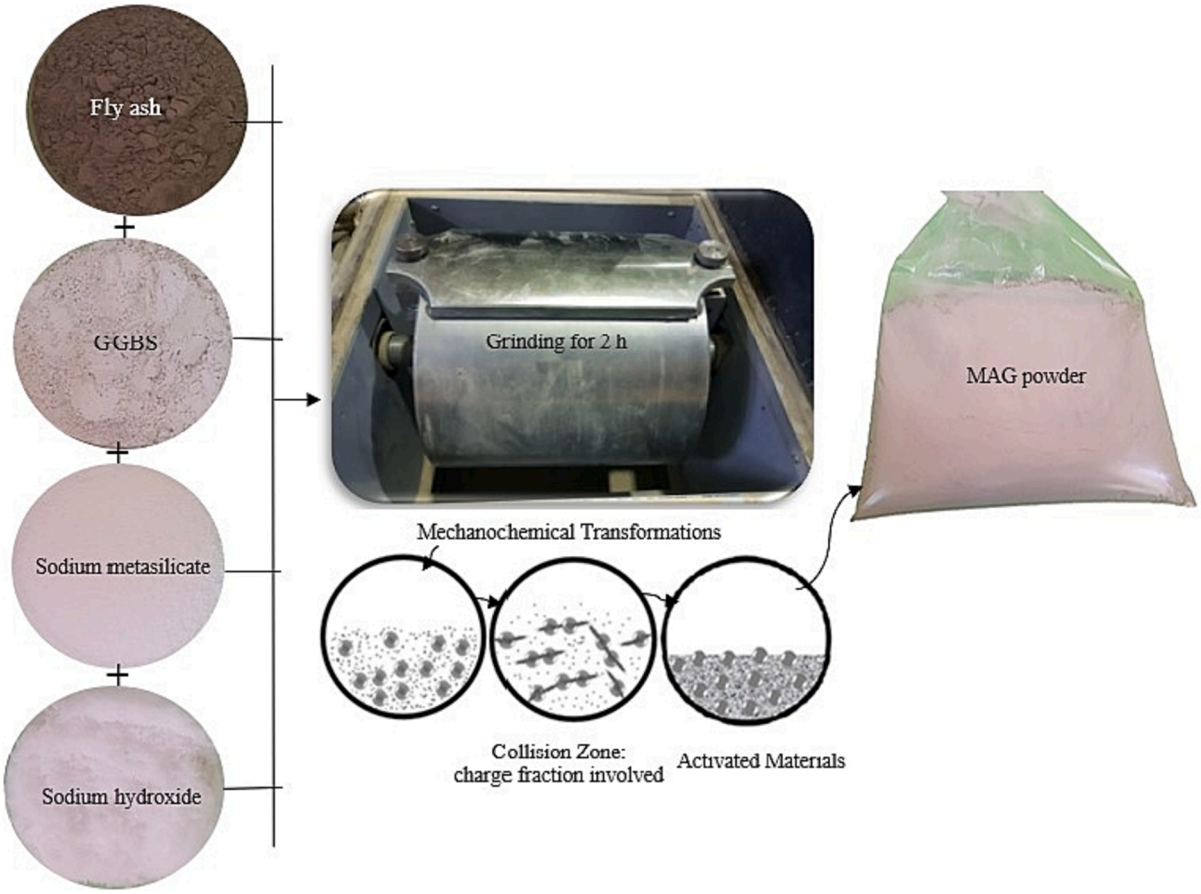

Fig. 2. The manufacturing process of MAG powder.

containing four GGBS ratios (0 %, 50 %, 75 %, and 100 %). For instance, the CAG-100S code indicates that the adopted slurry is a geopolymer that has been conventionally activated, including 0 % fly ash and 100 % GGBS. Also, the MAG-75S code denoted that the geopolymer type is a mechanochemically activated geopolymer binder containing 25 % fly ash and 75 % GGBS. Table 3 displays the mixture proportions of both MAG- and CAG-stabilized soils.

Test methods

All specimen preparation and testing were conducted in the laboratory at room temperature. The mixing procedure adopted for preparing the specimens was uniform for all the tests. First, the oven-dried soil and water were separately weighed and mixed in a container to set the moisture content of the remoulded soil to 36 % (LL-5). This moisture content was chosen to simulate soft soil. According to previous studies (Güllü et al., 2017; Pakbaz and Farzi, 2015; Bhadriraju et al., 2008), deep mixing treatment is mostly applied for soils where the water content is close to the liquid limit.

The remoulded soil was carefully placed into sealed bags and allowed to sit for 24 h to guarantee sufficient contact between the soil particles and moisture. The mixing procedure for obtaining grout mix samples followed the method reported by Hamid Abed et al., (2022b, 2022c). Based on previous research (Arulrajah et al., 2018; Chew et al., 2004), it has been found that soil can be effectively stabilized when the dosage of the stabilization agent is in the range of 20–30 % of the dry soil mass. Therefore, the dry material of the stabilization agent was set at 30 % of the dry soil mass, and the water-to-binder ratio was set at 1. The remoulded geopolymer-stabilized soil (MAG and CAG) was mixed using a mixer at a speed of 240 rpm for 3 min, ensuring thorough stirring to form geopolymer-stabilized soil. The mixture was then poured into cylindrical moulds with a diameter of 50 mm and a height of 100 mm. To

Table 3
Mix proportions deep mixing soil.

MixID	geopolymer slurry						Soil	
	FA (g)	GGBS (g)	NaOH (g)	Na_2SiO_3 (g)	Grinding duration: h	Water (g)	Clay (g)	Clay moisture content (%)
CAG-0S	850	0	100	50[a]	–	1000	3333.3	36
CAG-50S	425	425	100	50[a]	–	1000	3333.3	36
CAG-75S	212.5	637.5	100	50[a]	–	1000	3333.3	36
CAG-100S	0	850	100	50[a]	–	1000	3333.3	36
MAG-0S	850	0	100	50[b]	2	1000	3333.3	36
MAG-50S	425	425	100	50[b]	2	1000	3333.3	36
MAG-75S	212.5	637.5	100	50[b]	2	1000	3333.3	36
MAG-100S	0	850	100	50[b]	2	1000	3333.3	36

[a]Composed of the sodium silicate activator (in liquid form).
[b]Composed of sodium metasilicate -Penta" activator (in powder form).

minimize experimental errors, three parallel samples were prepared for each group. The geopolymer-stabilized soil specimens were vibrated after each filling for 10–20 s to remove any air bubbles that may have formed during the specimen preparation process. Subsequently, curing of the geopolymer-stabilized soil specimens occurred at temperatures within the range of 20 to 26 °C in well-sealed plastic bags until the designated curing time was reached.

The UCS tests of the DSM specimens were conducted by uniaxial loading at a loading rate of 1 mm/min. The UCS value was calculated by taking the peak axial stress measured at the point of failure into consideration. It should be noted that before performing the UCS tests, the geopolymer-stabilized specimens were utilized to quantify the wave velocity (UPV) according to ASTM C597–09 (Astm, 2009). The ultrasonic pulse velocity test, classified as a non-destructive test, was utilized to assess the stiffness of the hardened materials. The magnitude of UPV measures can be interpreted based on several classifications from previous research (Anon, 1979) (Table 4).

To characterize the microstructure and chemical composition of the materials, scanning electron microscope (SEM) analysis was conducted using a ZEISS Gemini SEM 300. The raw materials, geopolymer precursors generated from the mechanochemical grinding process, and the hardened geopolymer-stabilized soil were subjected to SEM inspection. Additionally, X-ray diffraction (XRD) was used to evaluate the crystalline structure of the geopolymeric powder qualitatively before the mechanochemical activation process and after it ceases. Furthermore, Fourier transforms infrared (FTIR) spectroscopy was conducted in the spectral range of 450 to 2000 cm^{-1} to identify the chemical bonds present in the hardened geopolymer-stabilized soil. These analytical techniques were utilized to gain insights into the microstructural and chemical characteristics of the geopolymer materials and their performance after the activation process.

The test for sulfate attack is conducted in a similar way as that reported by Kamon et al., (1993). Each of the specimens cured for 28 days was submerged in a 1 % magnesium sulfate solution for up to 120 days, while control samples (unexposed) of the same mixtures were stored at room temperature until testing age. Before the exposure to the $MgSO_4$ solution, both MAG and CAG-stabilized soil samples were soaked in water for one day and then dried for two hours at a temperature of 23 °C to determine their initial mass. Every 15 days during the exposure period, samples were collected from the magnesium sulfate solution tank and washed with water to eliminate any chemical reaction products that precipitated on the exposed samples' surface. The stabilized soil specimens were then dried for 2 h at 23 °C before being weighed. The magnesium sulfate is replenished every 15 days in all cases. Various tests, including visual inspection, mass change, UCS, and UPV loss, were conducted at regular intervals throughout the duration of exposure to determine the impact of $MgSO_4$ solution on geopolymer-stabilized soil samples. The percentage change in mass was also calculated by the mass change between the exposed samples and corresponding unexposed samples compared to the mass of unexposed samples. Before conducting strength tests, stabilized soil specimens were visually inspected for symptoms of deterioration, such as cracking, spalling, and delamination.

Table 4
Ultrasound Pulse Velocity (UPV) classification (Anon, 1979).

Ultrasound Pulse Velocity (m/s)	<2500	2500–3500	3500–4000	4000–5000	>5000
Label	Very low velocity	Low velocity	Moderate velocity	High velocity	Very high velocity

Results of the present work and their discussion

Microstructure analysis of geopolymeric precursor

Fig. 3 depicts FA and GGBS particle size distribution before and after the mechanochemical activation process. The D50 of the median size of raw GGBS and fly ash particles were 22 μm and 38 μm, while dropped to 15 μm and 20 μm, respectively, after 2 h of mechanochemical synthesis with solid alkali activators in ball milling.

The changes in the microstructure of FA and GGBS antecedents before and after mechanochemical synthesis with solid alkali activators were analyzed using SEM. The majority of the raw FA particles were observed to be spherical in shape, as depicted in Fig. 4a. However, post-to co-grinding FA with solid alkali activators for a duration of 2 h, the average particle size of both the solid compounds and FA decreased. However, some fine-grained particles agglomerated, and the raw FA retained its spherical shape to some extent. Moreover, the combination of sodium metasilicate and sodium hydroxide resulted in the initial binding of FA particles (Fig. 4b). Gupta et al., (2017) found that ball-grinding FA and sodium hydroxide for 8 h increased surface area and reaction rate by creating cracks and defects. Fig. 4c-d displays SEM images of raw GGBS and mechanochemically synthesized GGBS precursors. The size and shape of GGBS granules in Fig. 4c were heterogeneous and dissimilar, with sub-rounded to angular shapes and rough edges and bulk, as observed by Baalamurugan et al., (2021). After undergoing 2-hour mechanochemical processing (Fig. 4d), the size of GGBS particles was generally reduced, while their angular and deformed shapes remained intact. Furthermore, this process increased the particles' surface area and expedited the reaction rate of the geopolymer antecedents.

XRD spectra of the raw geopolymeric (G-100S) powder and mechanochemical activation geopolymeric (MAG-100S) precursors are plotted in Fig. 5. The MAG-100S powder samples were co-grinded GGBS with sodium metasilicate and sodium hydroxide. The G-100S powder was formed of manually dry-blended GGBS, sodium metasilicate, and sodium hydroxide, with no grinding. The geopolymeric precursor (G-100S) exhibits a vitric structure with an amorphous phase, as indicated by a bulge between 28° and 33° (2θ value) with a 30° spike. In addition, crystalline phases are depicted in Fig. 5 by sharp peaks made up mostly of calcium silicate, gehlenite, akermanite, and merwinite, as seen by the high peaks between $2\theta = 15°$ and $2\theta = 90°$ (Zhang et al., 2008; Yusuf et al., 2014). The X-ray diffraction (XRD) pattern analysis of the co-grinded (MAG-100S) and raw (G-100S) antecedents (Fig. 5) revealed that the peak intensity of the co-grinded antecedent was considerably weaker than that of the raw antecedent, indicating that the crystalline phases of the GGBS had amorphized due to the mechanochemical grinding process using NaOH and sodium metasilicate. The disorder and surface area were increased by the mechanochemical activation process, which promoted the reaction between the raw powders (Gupta et al., 2017). These results demonstrate that the mechanochemical grinding process effectively transformed the crystalline phases of the GGBS into an amorphous state, thereby facilitating the subsequent geopolymerization process.

Strength performance of DSM

The UCS values of DSM (MAG and CAG) samples at various GGBS contents are seen in Fig. 6. It is noticeable that the UCS values obtained in this study meet the minimum strength requirements (>0.4 MPa) for bearing capacity in ground improvement applications according to Coduto et al., (1999). This indicates that the geopolymer-stabilized soil samples prepared in this study have the potential to be used as a suitable alternative to traditional cement-stabilized soil in ground improvement applications (Güllü and Ali Agha, 2021).

The mechanical properties of DSM samples were found to be significantly influenced by the mechanochemical activation of the

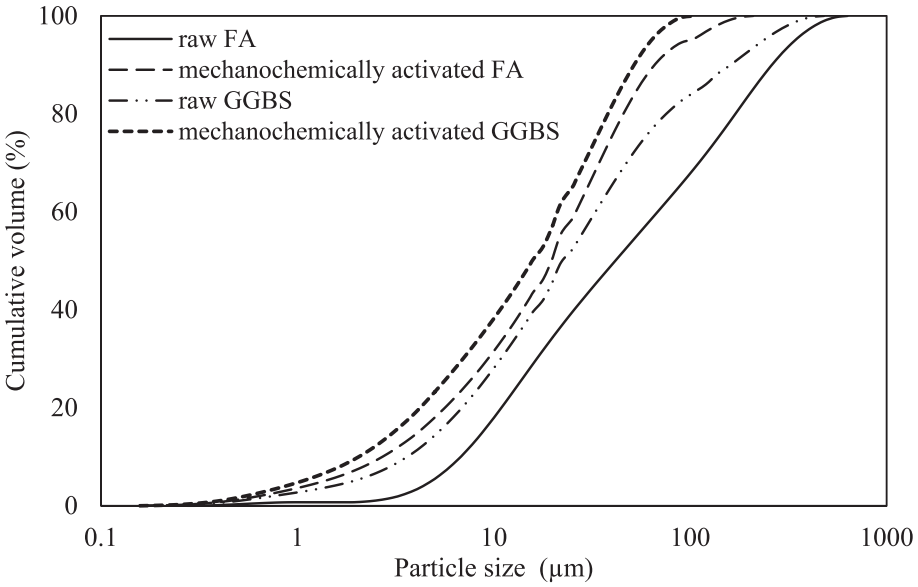

Fig. 3. The grain size distribution of the raw and mechanochemically activated FA and GGBS.

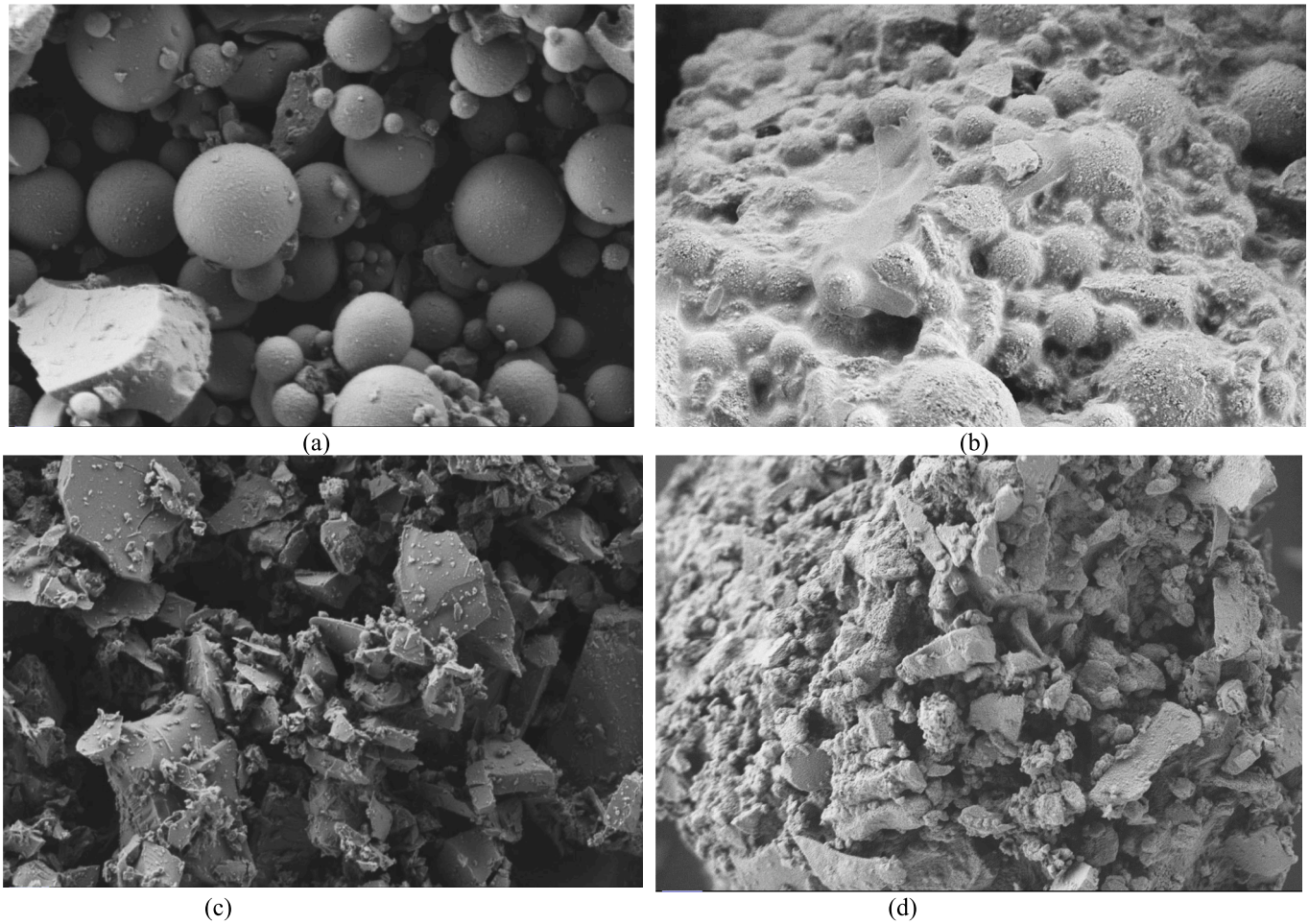

Fig. 4. SEM images of (a) raw FA, (b) mechanochemically activated FA, (c) raw GGBS, and (d) mechanochemically activated GGBS.

geopolymer binder, as demonstrated by the experimental results. The UCS of MAG samples exhibited a strength increase of approximately 12 %, 11 %, 45 %, and 23 % for MAG-0S, MAG-50S, MAG-75S, and MAG-100S, respectively, when compared to its conventionally activated geopolymer counterpart. The mechanochemical synthesis of the geopolymer binder was responsible for the enhanced strength of MAG-stabilized soil samples. According to Hamid Abed et al., (2022a), the mechanochemical activation process enhanced the surface area and

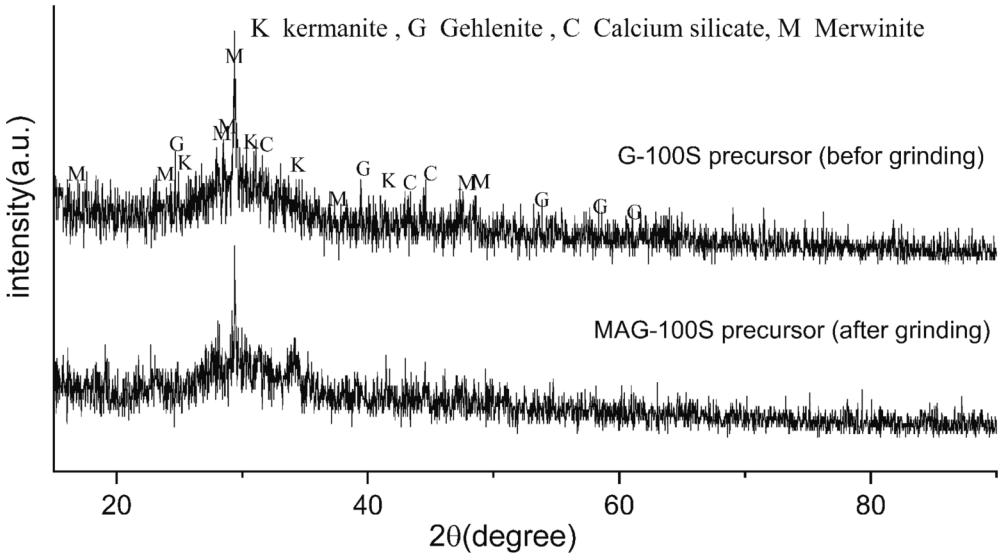

Fig. 5. X-ray diffraction of G-100S and MAG-100S precursor.

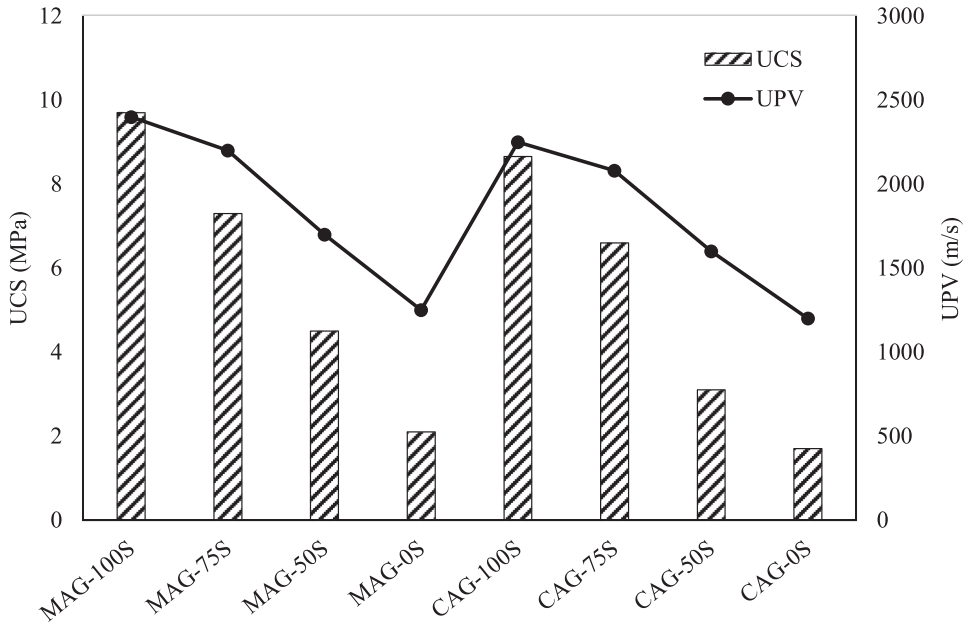

Fig. 6. UCS and UPV of MAG and CAG- stabilized soil specimens.

reactivity of the geopolymer binders, resulting in the formation of more gel within the geopolymer-stabilized matrix, and the total pore volume and porosity decreased, thereby strengthening the bond between soil particles and leading to an increase in the strength of the MAG soil sample. As depicted in Fig. 6, the UCS of DSM samples increased proportionally with the GGBS content, where the UCS of the MAG-50S, MAG-75S, and MAG-100S samples increased by 114 %, 247 %, and 361 %, respectively, compared to the sample containing 100 % FA. GGBS's superior cementing properties and higher reactivity, as compared to FA, are the primary reasons for its significant impact on UCS Hamid Abed et al., (2022b, 2022c). Furthermore, the high CaO content plays an important function in enhancing activation and early-age strength (Nath and Kumar, 2013). The enhancement in mechanical properties with the increase in GGBS content is also consistent with the literature on alkali-activated FA/GGBS-stabilized soil where an increase in UCS with the increase in GGBS content is reported by Luo et al., (2022), Zhao et al., (2007) and, Lee and Lee, (2013). This is linked to the creation of C-S-H/CA-S-H and C-A-S-H gels that condense the microstructure and reduce the porosity of the geopolymer-stabilized soil. The high CaO content in the GGBS promotes the formation of these gels, thereby modifying the microstructure and enhancing the mechanical properties of the geopolymer-stabilized soil (Nath and Kumar, 2019).

As illustrated in Fig. 6, UPV test was performed for both MAG, and CAG stabilized soils to validate the unconfined compressive strength values. The UPV values fall within the range of 1200 to 2400 m/s, corresponding to the very low-velocity degree described in (Anon, 1979) (Table 4). This low strength and UPV quality may be attributable to the clayey soil employed in this investigation (Güllü et al., 2017).

Fig. 6 shows that the UPV values are significantly affected by the activation method of the geopolymer binder, as established by the present results. The UPV of MAG-100S, MAG-75S, MAG-50, and MAG-0S were 2400, 2200, 1700, and 1250 while the UPV of CAG-100S, CAG-75S, CAG-50S, and CAG-0S was 2250, 2080, 1600, and 1200 m/s respectively (Fig. 6). The reduction in particle size and the increase in

surface area of geopolymeric particles, resulting from the grinding process of the source material during the mechanochemical processing, lead to a decrease in porosity and an increase in density of geopolymer stabilized soil Hamid Abed et al., (2022b, 2022c). Therefore, it can be inferred that the mechanochemical synthesis outperforms the traditional activation method in terms of enhancing UPV values.

Regarding GGBS replacement, the results reveal that the UPV values follow a similar trend to that of the UCS results. As shown in Fig. 6, the UPV values of both the MAG and the CAG samples have increased with the increase in GGBS content. The UPV values of MAG-50S, MAG-75S, and MAG-100S increased by 36 %, 76 %, and 82 % compared to the MAG-0S. This is mostly owing to the increased availability of geopolymer gel to more effectively bind the soil particles, leading to an increase in the density of the DSM samples and, consequently, an increase in the UPV value (Kumar et al., 2010).

Microstructural analysis of DSM

Fig. 7 depicts the effect of the activation method and GGBS substitution on the microstructure characterization of the geopolymer-stabilized soils. Fig. 7 illustrates that the soil stabilized by mechanochemically activated geopolymer exhibited a denser and more compact performance compared to the soil stabilized by conventionally activated geopolymer. Furthermore, unreacted particles are more evident in CAG-stabilized soil, which developed less C-S-H gel and resulted in a loose microstructure, in contrast to MAG-stabilized soil, which appeared to be well-connected by a gel-like network. According to Hamid Abed et al., (2022c) and Abbas et al., (2022), the mechanochemical activation process increased the surface area and reactivity of the geopolymer stabilizer, resulting in the formation of more gel within the geopolymer-stabilizer matrix. As a result, the total pore volume and porosity decreased, strengthening the bond between soil particles and resulting in an improvement in the microstructure characterization of the stabilized soil sample.

Besides, the increase in slag content significantly affected the microstructure properties of the geopolymer-stabilized soil. As shown in Fig. 7(a and c), the SEM image of both CAG and MAG -stabilized samples became more compact and homogeneous when fly ash was substituted with GGBS. This explains the significant concomitant increase in observed strength values. It could be ascertained that the geopolymer-stabilized samples containing 100 % GGBS had a more compact, homogeneous structure with produced gels and less of particles that did not contribute to the reaction (Fig. 7a and c) than the counterpart of samples containing 50 % FA (Fig. 7b and d), which show a more porous and less cohesive microstructure.

Previous studies by Abdullah et al., (2019) and Luo et al., (2022) have shown that soil samples with high GGBS content are efficiently activated by the alkali activator, resulting in the formation of homogenous geopolymer gels, including net-like or interlocking C-A-S-H and platy C-S-H, that encase soil particles and result in denser internal

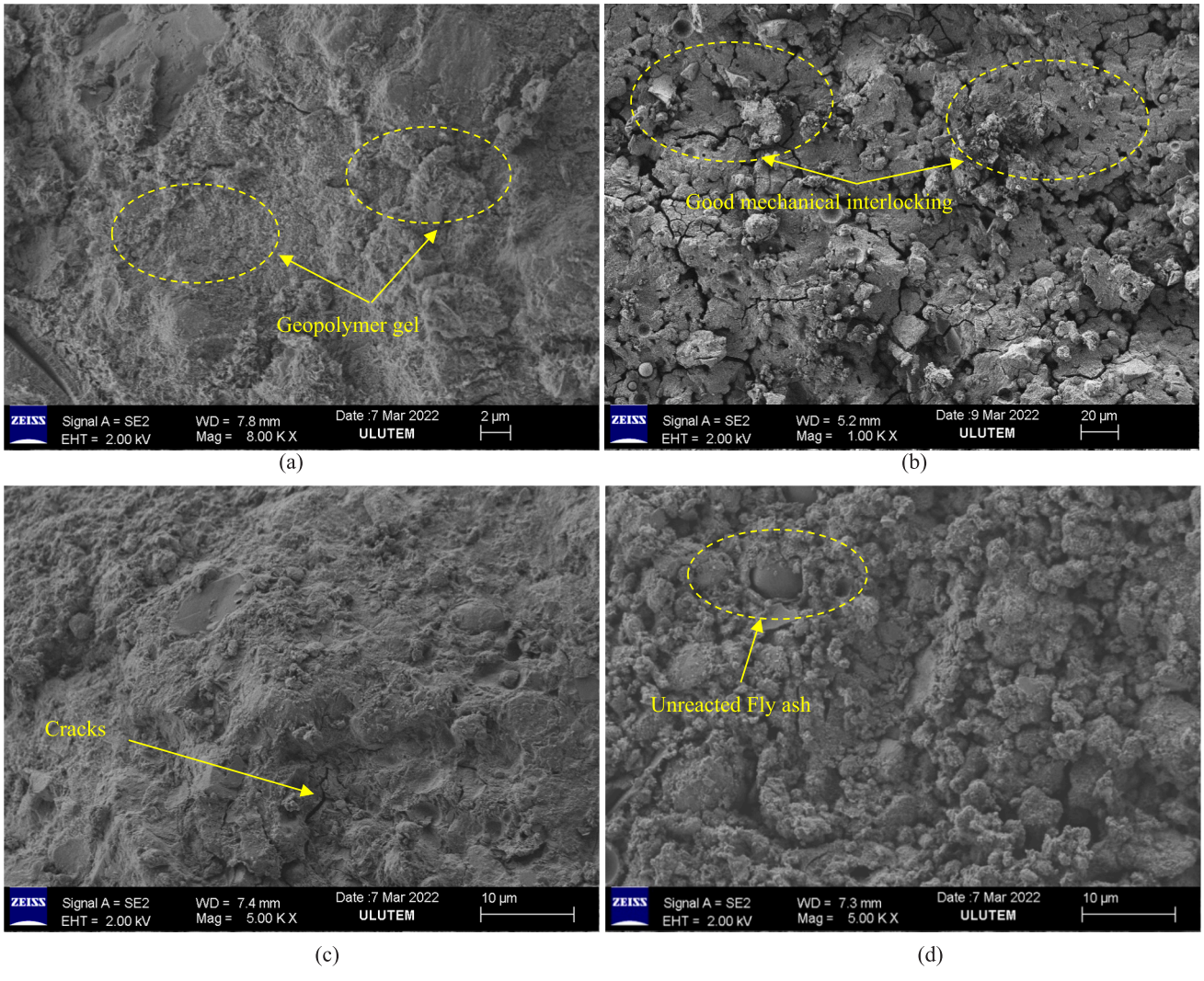

Fig. 7. SEM images of geopolymer-stabilized soil;(a) MAG-100S;(b) MAG-50S;(c) CAG-100S; and (d) CAG-50S.

structures. As a result, the macroscopic strength of the soil is increased. Conversely, an increase in FA content, up to 50 %, results in the presence of unreacted spherical FA particles that work like mineral additives. These additives occupy space within the sample and increase its porosity, as depicted in Fig. 7c. Furthermore, the study conducted by Luo et al., (2022) revealed that an increase in FA content causes N-A-S-H to have a higher inhibitory effect on GGBS hydration. This, in turn, reduces the cohesiveness of the geopolymer gel on soil particles and amplifies the porosity of the samples.

Fourier Transform Infrared Spectroscopy (FTIR) was utilized in this study to investigate the impact of the activation method and FA /GGBS ratio on the characteristics of DSM samples (Fig. 8). FTIR spectroscopy is a chemical technique that allows for the investigation of the rate of formation and geopolymerization of reaction products in various geopolymer-stabilized soil samples (Ryu et al., 2013). The analysis focused on identifying the reaction zones of Al-O and Si-O through distinct spectral zones, including those located at 1100–900 cm^{-1} that correspond to the asymmetric stretching vibration of (Si-O-Al) and (Si-O-Si), the bands at around 2000 cm^{-1}, which are related with the stretching vibrations of H–O–H bonds, and the band situated around 1650 cm^{-1}, which is linked with the bending vibration of the –OH groups of hydrated reaction products in water (Nath and Kumar, 2013; Al-Majidi et al., 2016).

According to Fig. 8, the vibrational component bands of the MAG and CAG stabilized soils in the FTIR spectrum differed. The variation in the values of peaks is associated with the structural reorganization owing to the activation mechanism (Hosseini et al., 2021). It is important to note that a significant difference was observed in the low-frequency range (1000–500 cm^{-1}), where a large number of bands appeared, which is a characteristic region of amorphous Si-Al bonds. The DSM samples prepared using a mechanochemically activated geopolymer binder exhibited an increase in the intensity of IR peaks, indicating greater polymerization (Kumar and Kumar, 2011). Furthermore, the emergence of these bands suggests the formation of three-dimensional ring interconnections, which is associated with the higher strength performance of the MAG-stabilized soil, as reported by Gupta et al., (2017). In addition, the FTIR spectra also reveal that the peaks associated with the bending vibration of –OH groups of hydrated reaction products in water decrease in intensity as the proportion of GGBS to FA increases, indicating a decrease in the amount of unreacted FA particles and the formation of a more homogeneous geopolymer gel structure (Ryu et al., 2013). This is in accord with the results of the strength tests, which show that higher GGBS content results in higher strength performance (Al-Majidi et al., 2016).

Durability studies

Visual appearance

Figs. 9 and 10 show the visual inspection of DSM (MAG and CAG) specimens exposed to 1 % magnesium sulfate over 60 and 120 days with varying GGBS to FA ratios. Control samples (unexposed) were also displayed for comparison purposes. It is important to notice that samples containing 100 % FA experienced significant deterioration, as demonstrated by the occurrence of substantial scaling and spalling in the MAG-0S and CAG-0S stabilized soil samples after 60 days of being exposed to magnesium sulfate. After 120 days of being exposed, complete damage was observed, making it impossible to continue further exposure due to the severity of the damage (Figs. 9 and 10). On the other hand, many visible corrosion layers spalling were seen in all the geopolymer-stabilized soil samples after immersion in a magnesium sulfate solution. The CAG-50S sample exhibited a surface colour change, severe deterioration with the corroded layer obviously spalling, and cracks appearing around the edge. This suggests that adding FA renders the binders more susceptible to $MgSO_4$ degradation. The stabilized soil with 75 % and 100 % GGBS content remained intact even after the 120-day exposure to magnesium sulfate solution, indicating a stronger sulfate attack resistance than the 100 % FA samples. The presence of GGBS, which is the major source of Ca (Table 2), compacts the mixes and provides a greater density due to the development of additional geopolymerization products since geopolymers containing GGBS contain gels (C-A-S-H), hence decreasing void ratio and sulfate absorption. Several earlier investigations (Elyamany et al., 2018; Garcia-Lodeiro et al., 2011; Deb et al., 2014) support this explanation. The effect of the activation mechanism on the visual inspection of MAG and CAG samples exposed to 1 % magnesium sulfates for 60 and 120 days was depicted in Figs. 9 and 10. The CAG samples exhibited minimal visible

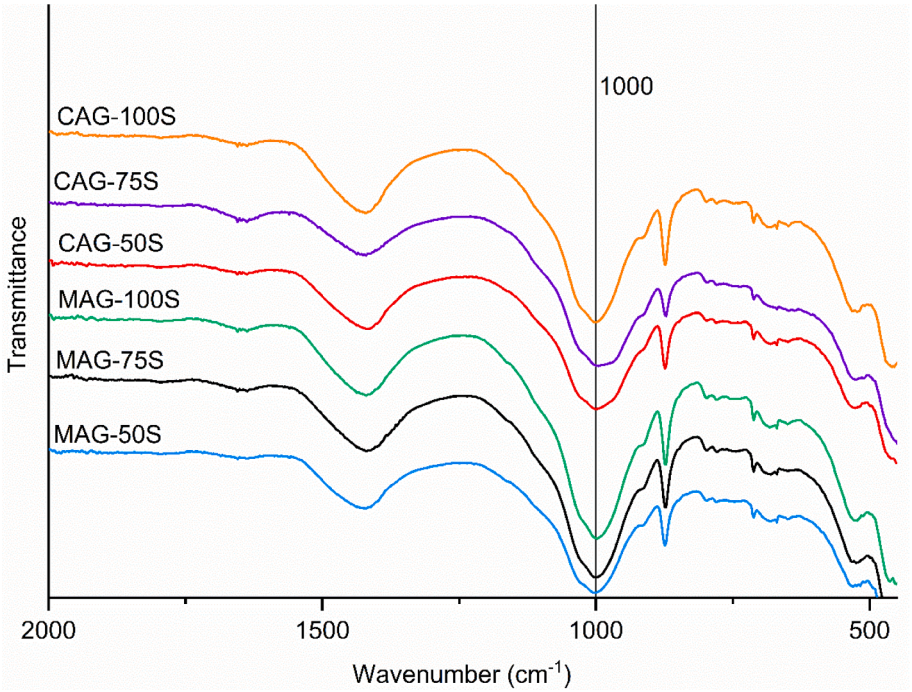

Fig. 8. FTIR spectra of MAG and CAG- stabilized soil.

damage and appeared to remain structurally sound, with only minor erosions observed at the corners and regions near the edges after 60 days (except CAG-0S). However, specimens subjected to magnesium sulfates undergo colour changes due to the formation of a white covering approximately 1 mm thick on their surfaces, as seen in Fig. 9. This also aligns with the results published by Salami et al., (2017). According to Ye et al., (2019), the white colour of samples was mainly ascribed to the generation of gypsum and ettringite. As the exposure progresses, the CAG-stabilized soil samples display substantial degradation against sulfate attack, manifesting as surface erosion, expansion, and surface cracking after 120 days compared to the control specimens. In other words, the amount of erosion increased as exposure duration increased. This chemical change is commonly linked to the crystallization pressures generated by the development of salts (ettringite, gypsum) that increase with exposure duration (Helson et al., 2018).

In contrast, MAG-stabilized soil samples exposed to magnesium sulfate solution demonstrated minimal sulfate degradation and no apparent deterioration or surface spalling at both 60 and 120 days. Due to the fact that mechanochemical synthesis of source material boosted the reactivity of source materials, more gel was produced as the principal reaction product, which filled the pore system and decreased sulfate attack penetration. In comparison, all CAG- stabilized soil samples subjected to $MgSO_4$ solution proved to be damaged severely, with the corroded layer spalling, and cracks appearing around the edge. This

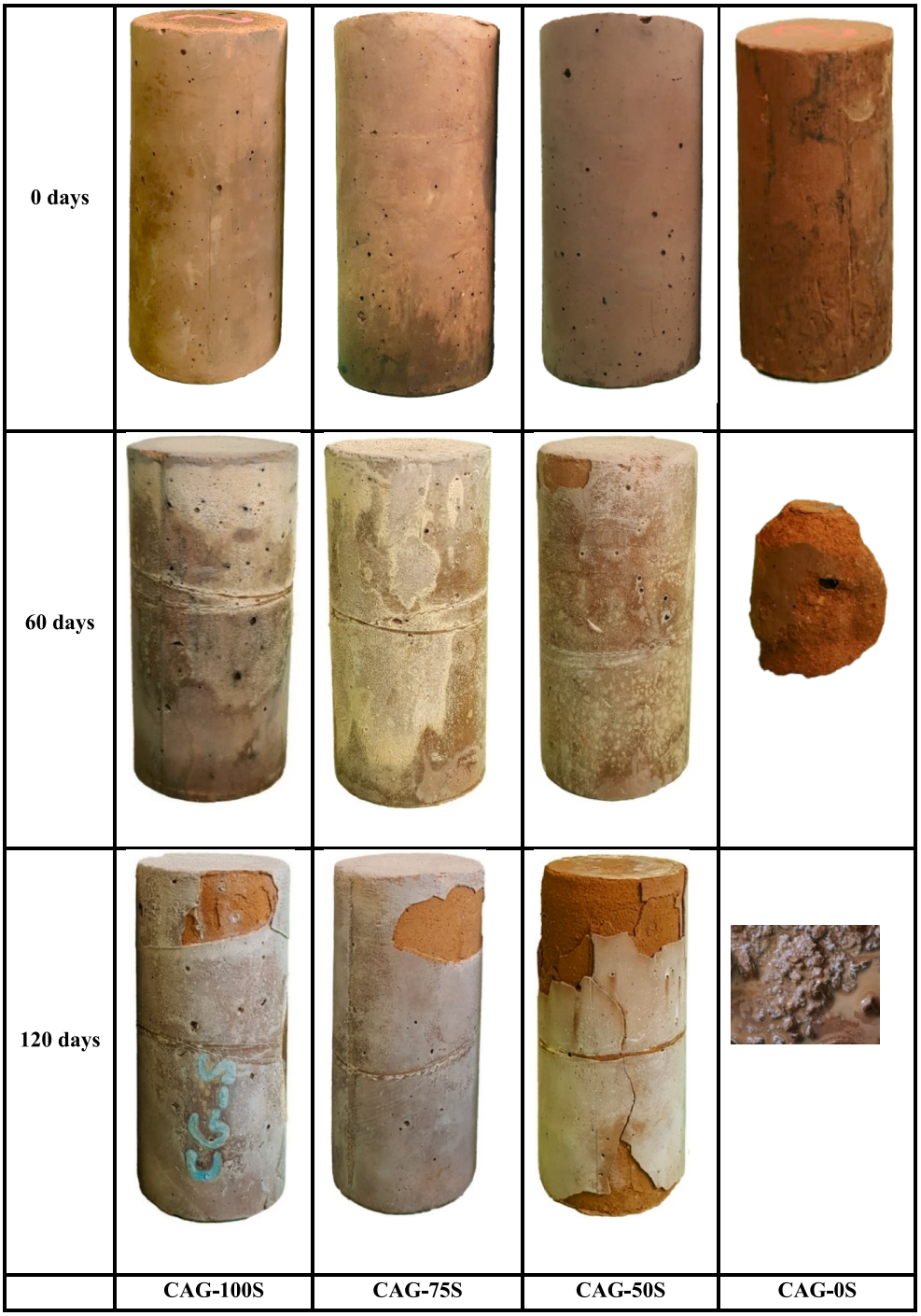

Fig. 9. The visual appearance of CAG- stabilized soil samples exposed to 1 % $MgSO_4$ solution for 0, 60, and 120 days.

indicates that the conventionally activated geopolymer binders were more prone to $MgSO_4$ attack (Fig.10).

Mass change

Fig. 11 depicts the mass change of DSM (MAG and CAG) samples stored at room temperature. The results showed that all DSM samples exhibited mass loss when stored at ambient temperature for up to 120 days. The DSM samples lose weight over time due to the evaporation of water present in the sample during ambient curing. However, the mass loss of MAG samples was lower than that of CAG samples stored at ambient temperature. The mass loss of MAG-100S and MAG-0S samples was −2.29 % and −5.2 %, respectively, while it was −2.92 % and −5.8 % for CAG-100S and CAG-0S samples after 120 days. Mechanochemical activation enhanced the geopolymer binder's surface area and reactivity, resulting in more gel filling the pore system and preventing water evaporation, resulting in weight retention over time. On the other hand, the percentage of mass loss decreases as the GGBS content increases, as seen in Fig. 11. The weight reduction was −5.8 %, −3.77 %, −3.19 %, and −2.92 % for CAG samples with FA contents of 0 %, 50 %, 75 %, and 100 %, respectively, at 120 days. The high porosity of FA particles causes significant mass loss in DSM samples containing a high proportion of FA (see Fig. 7d). Gopalakrishnan and Chinnaraju, (2019) found that geopolymer samples containing full GGBS had a lower mass loss under ambient curing than samples containing 100 % FA.

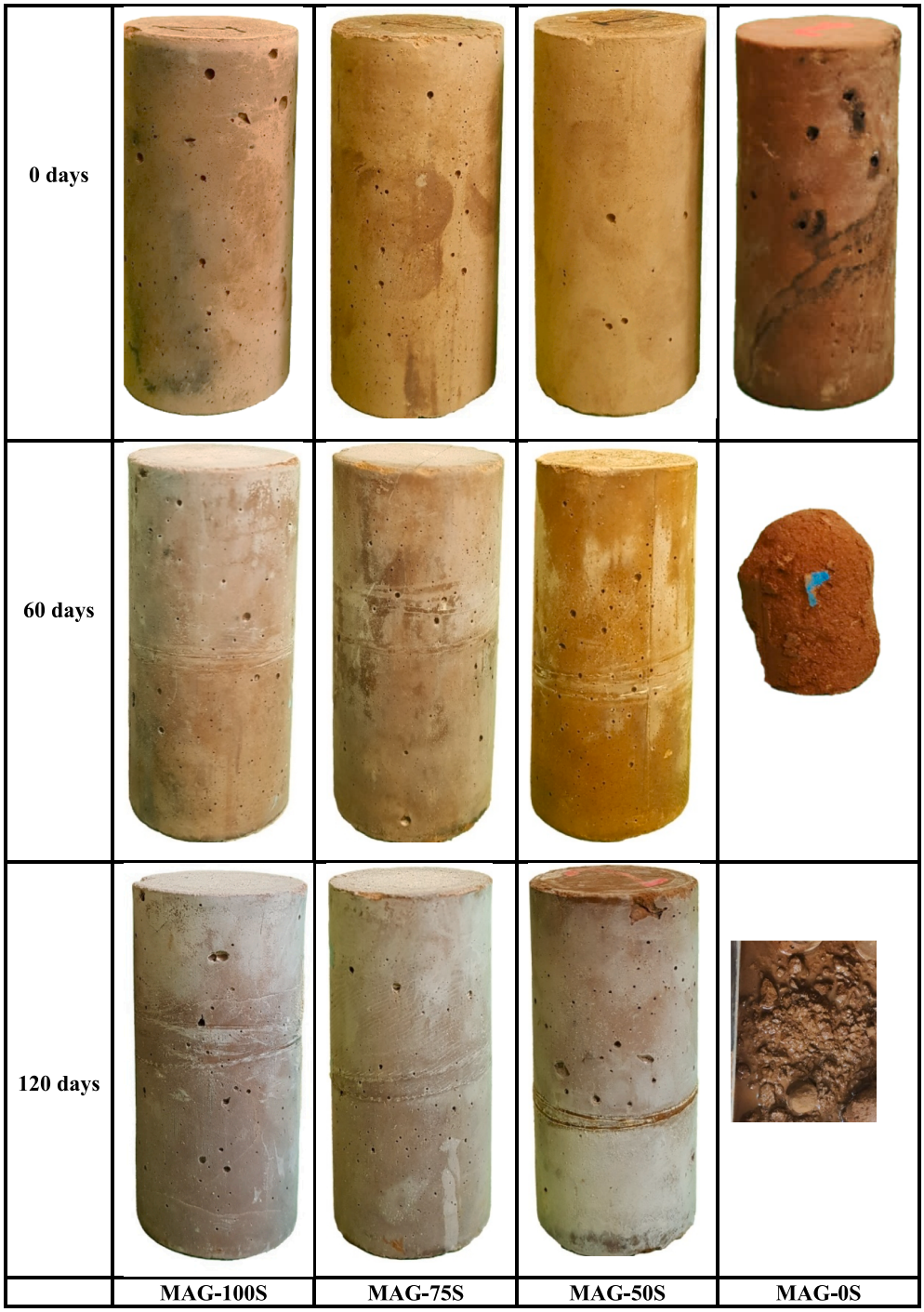

Fig. 10. The visual appearance of MAG-stabilized soil samples exposed to 1 % $MgSO_4$ solution for 0, 60, and 120 days.

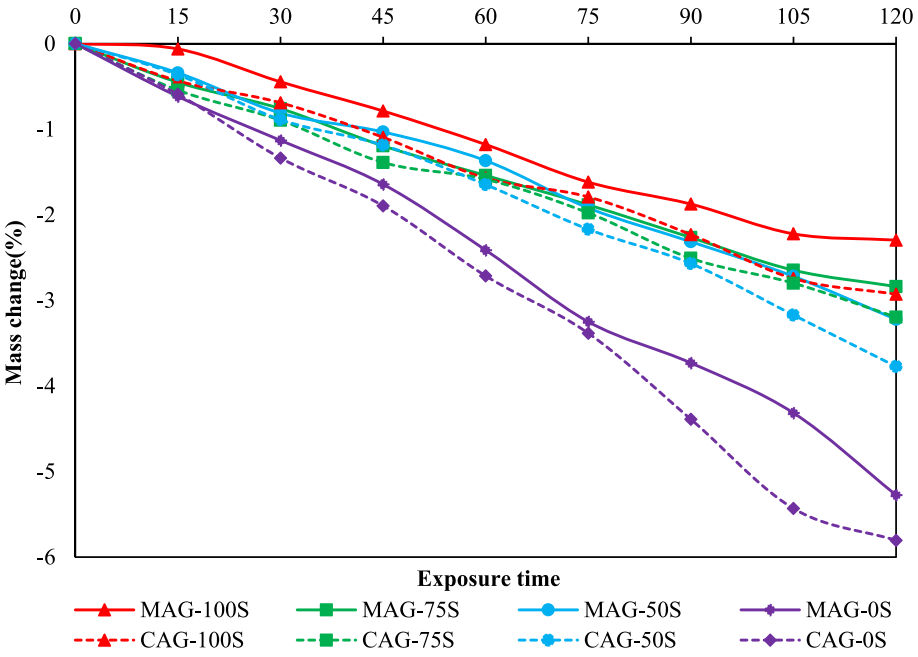

Fig. 11. Mass change of MAG and CAG- stabilized soil specimens stored at ambient temperature.

The mass change percentages of MAG and CAG-stabilized soil samples with various ratios of GGBS to FA subjected to magnesium sulfate solutions are depicted in Fig. 12. At the same immersion period, it was observed that the CAG-stabilized soil had more mass change than the MAG-stabilized soil. After 120 days of exposure to magnesium sulfates, the mass changes of MAG-50S, MAG-75S, and MAG-100S samples were + 0.3 %, +0.75, and 16 %, respectively, while their CAG counterparts were + 0.75 %, +0.1, and −0.87 %. (Fig. 12). The different performance in mass between CAG and MAG was due to the difference in the activation method of geopolymer binder, where mechanochemical synthesis processing enhanced the surface area and reactivity of geopolymer binder and led to the development of more gel as the primary reaction product (Abbas et al., 2022), which lowered the porosity and raised the density of MAG-stabilized soil (Hamid Abed et al., 2022c), thereby reducing the penetration of magnesium sulfate into the pore structure of the MAG sample, resulting in increased resistance to sulfate attack compared to CAG stabilized soil.

Notably, the sample containing 100 % FA, regardless of geopolymer type (MAG-0S and CAG-0S), exhibits a significant decrease in mass at 60 days, while the mass fully disintegrates after 120 days of exposure to magnesium sulfate (Fig. 12). Conversely, DSM samples gain mass after soaking in magnesium sulfate solution when GGBS replacement exceeds 50 %, and this mass gain increases with exposure duration (except the CAG-50S mix shows a drop in mass after 60 days). The observed mass gain in the soil samples could be ascribed to the chemical reaction between the sulfate ions present in the solution and the cementitious

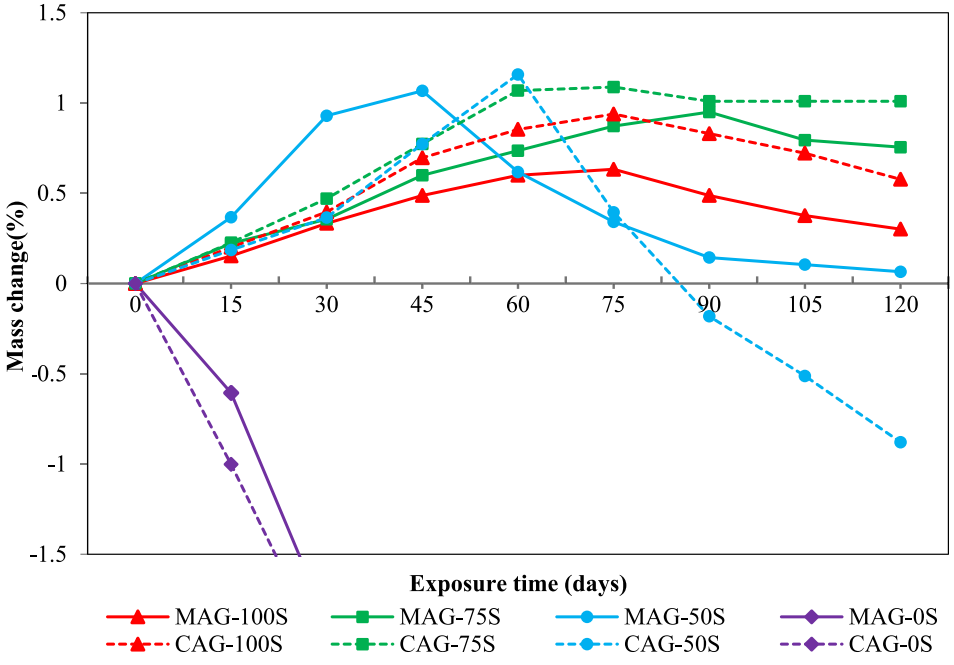

Fig. 12. Mass change of MAG and CAG- stabilized soil specimens exposed to 1% $MgSO_4$ solution.

elements in the soil, including C-S-H, C-A-H, CA-S-H, and Ca $(OH)_2$. This reaction leads to the formation of ettringite, thaumasite, and gypsum, which can increase the mass of the soil samples (Jiang et al., 2018). The formation of these sulfate minerals is associated with the consumption of calcium hydroxide and the subsequent depletion of this key component in the soil matrix. This chemical reaction can also lead to the formation of internal cracks in the soil matrix, which can further contribute to the observed mass gain (Tian and Cohen, 2000). Moreover, solution absorption into large voids interconnected in stabilized soils causes mass gain. This behaviour is consistent with Indu Siva Ranjani and Ramamurthy, (2012) findings about foam concrete. It is important to note that exposed samples containing 100 % GGBS experience less mass change than exposed samples containing 50 % and 75 % GGBS due to the lower density of FA relative to GGBS and the pores arising from unreacted FA particles. In contrast, the low mass change of specimens containing 100 % GGBS might be attributed to the higher fineness of GGBS, resulting in low porosity and high density, inhibiting magnesium sulfate solution absorption (Elyamany et al., 2018).

Strength loss

The residual unconfined compressive strength (UCS) of DSM specimens subjected to $MgSO_4$ solution for 0, 60, and 120 days is seen in Table 5 and Fig. 13. The results revealed that the residual UCS of DSM samples dropped when exposed to magnesium sulfate, and the rate of reduction increased as exposure time increased. The residual UCS-exposed MAG-100S and CAG-100S samples were 83 % and 79 % for 60 days, whereas more declined to 65 % and 60 %, respectively, after 120 days of immersion. The reduction in UCS of the DSM sample subjected to magnesium sulfate solution may be ascribed to the expansion of ettringite, thaumasite, and gypsum over time, which led to the formation of internal cracks within the soil. This remark is in accord with the findings of Bakharev, (2005), who demonstrated that the loss of strength in geopolymer materials when exposed to sulfate solutions is primarily due to the formation of internal cracks during immersion, mainly caused by the diffusion of Ca^{2+} into the sulfate solution. Regarding the activation method, the results indicate that the mechanochemical synthesis of the geopolymeric binder significantly affected the residual UCS values of geopolymer-stabilized soil samples after exposure to magnesium sulfate. As shown in Fig. 13, the residual UCS of MAG-50S, MAG-75S, and MAG-100S were 72 %, 25 % and 10 % higher than the counterparts of CAG-stabilized soil samples. It can be revealed that MAG samples performed better than CAG samples under magnesium sulfate attack due to the mechanochemical synthesis process of the geopolymeric binder, which reduced the particle size and increased the surface area of geopolymeric particles, thereby decreasing the porosity and raised the density of the geopolymeric binder. The low porosity of the MAG samples makes ionic species migration via the pore structure difficult and results in the least amount of deterioration during the test period. Also, the geopolymerization reaction rate of the MAG binder rose dramatically after grinding due to the development of more aluminosilicate gel in the mixture, which led to the creation of a more resistant structure against sulfate attack (Hamid Abed et al., 2022c). In addition, the increment in GGBS content substantially impacted the residual strength properties of geopolymer-stabilized soil specimens exposed to magnesium sulfate. The results revealed that DSM samples containing 100 % FA (regardless of geopolymer binder type) had no residual UCS (fully damaged), in contrast to specimens including 75 %-100 % GGBS, which had a higher UCS (Fig. 13). The residual compressive strengths for MAG-50S, MAG-75S, and MAG-100S samples were 40 %, 68 %, and 65 % when exposed to $MgSO_4$ solution for 120 days, respectively. The results indicated that samples with 75 % GGBS content demonstrated superior mechanical performance and durability resistance, while samples with 100 % GGBS content showed better durability resistance than those with 50 % GGBS content. Zhuang et al., (2016) observed that geopolymer samples with high FA content experienced significant degradation when exposed to $MgSO_4$ solutions as a result of the migration of Na^+ ions, which caused the formation of vertical cracks in the geopolymer mixture. Previous studies by Bonen and Cohen, (1992) and Nochaiya et al., (2010) have suggested that another potential explanation for this degradation is the migration of S and Mg from the magnesium sulfate solution into the matrix and the migration of Ca and alkalis from the interior of the sample to its surface. This migration can lead to the destruction of silicon-oxygen-silicon bonds in the aluminosilicate gel structure. As a result, sodium aluminium silicate hydrate (N-A-S-H) gels interact with $MgSO_4$ to produce magnesium aluminium silicate hydrate (M−A−S−H) gels with low strength. Despite the high CaO content in the MAG-100S and CAG-100S samples, these mixes exhibited a lower percentage of expansion compared to FA samples. This could be due to the consumption of CaO during the geopolymerization processes and hydration, resulting in a dense gel and strong cross-linked networks that reduce voids and fill pores in the gel. However, Gypsum crystals were also produced in MAG-100S, and CAG-100S stabilized soil specimens, which promote expansion but have a lower voids ratio than FA mixtures (Elyamany et al., 2018).

Ultrasonic Pulse velocity changes

Fig. 14 shows the variation in UPV for MAG and CAG-stabilized soil specimens after 0, 60, and 120 days of exposure to magnesium sulfate. Those results showed that the UPV measurements decreased with increasing exposure time to the $MgSO_4$ solution. The UPV values of CAG and MAG samples decreased by 16 % and 4 %, respectively, after 60 days of immersion in a sulfate solution, with further deterioration of 29 % and 25 %, after 120 days. UPV loss over time can be linked to the presence of micro-cracks caused by the development of ettringite and gypsum in the pores, as well as the migration of alkalis from geopolymers into the pores solution (Elyamany et al., 2018). This pattern is comparable to those found in earlier studies (Bakharev, 2005; Thokchom et al., 2010). As revealed in Fig. 14, the method of activation (mechanochemical processing) substantially impacted the UPV changes of MAG samples exposed to $MgSO_4$ solution. Those results demonstrated that MAG samples had a lower reduction in UPV values than CAG-stabilized soil specimens after 60 and 120 days of exposure to magnesium sulfate. For instance, The UPV values of MAG-50S, MAG-75S, and MAG-100S fell by 29 %, 22 %, and 25 % when exposed to magnesium sulfate for 120 days, whereas the UPV values of their CAG counterparts decreased by 41 %, 26 %, and 29 %. In other words, MAG specimens exhibited better magnesium sulfate resistance than CAG specimens. The high magnesium sulfate resistance of MAG-stabilized soil specimens was due to the mechanochemical activation, which increased the surface area and reactivity rate of the geopolymer binder, as well as the generation of more gel as the primary reaction product. This led to a reduction in porosity and an increase in density, resulting in a reduction in sulfate attack on MAG-stabilized soil specimens and a slight reduction in UPV (Hamid Abed et al., 2022b).

On the other hand, the increase in GGBS content played a crucial essential in minimizing the drop in UPV value of DSM samples subjected

Table 5
Residual unconfined compressive strength (%) of MAG and CAG-stabilized soil specimens exposed to 1% $MgSO_4$ solution.

Exposure time (days)	MAG-100S	MAG-75S	MAG-50S	MAG-0S	CAG-100S	CAG-75S	CAG-50S	CAG-0S
0	100	100	100	100	100	100	100	100
60	83	85	69	0	79	77	67	0
120	65	68	44	0	60	54	23	0

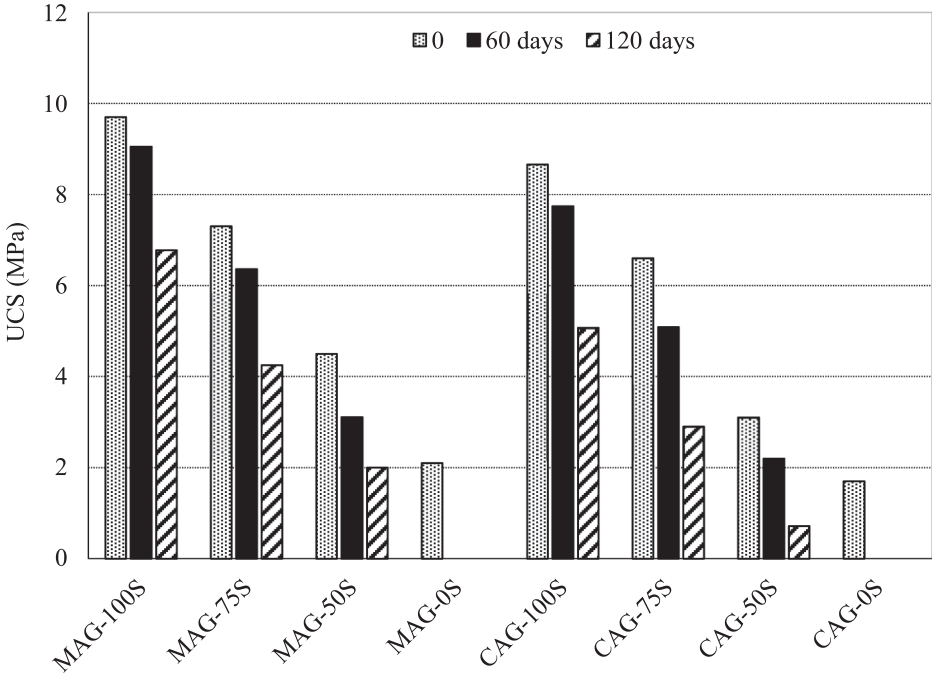

Fig. 13. Unconfined compressive strength of MAG and CAG- stabilized soil specimens exposed to 1 % $MgSO_4$ solution for 0, 60, and 120 days.

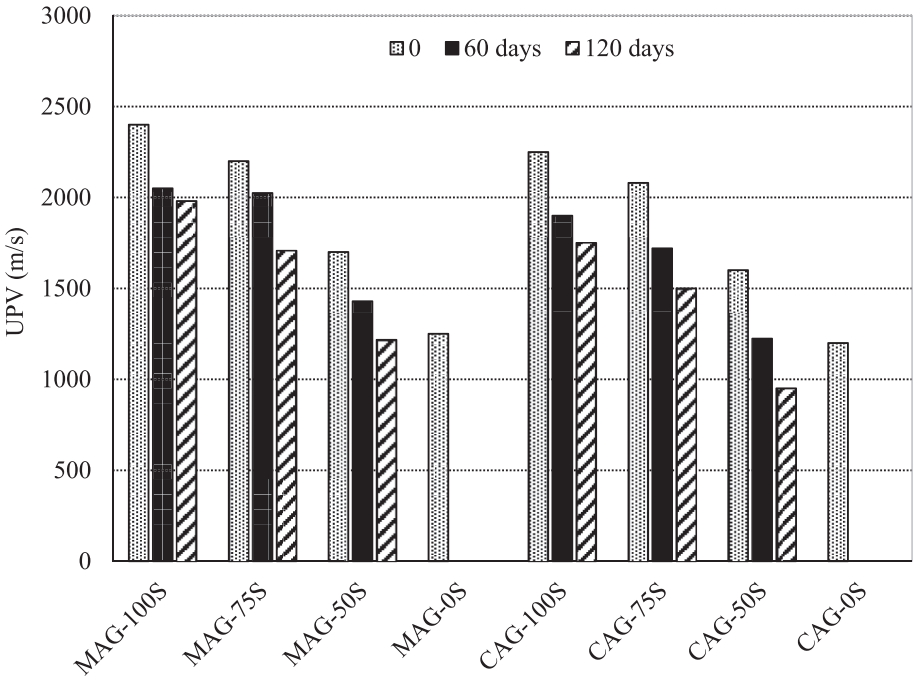

Fig. 14. Ultrasonic pulse velocity of MAG and CAG- stabilized soil specimens exposed to 1 % $MgSO_4$ solution for 0, 60, and 120 days.

to the $MgSO_4$ solution. The results indicated that samples with high GGBS content demonstrated the best mechanical performance and durability resistance, in contrast to the mixtures with high FA content showed low durability resistance. Fig. 14 shows that the UPV values of CAG-50S, CAG-75S, and CAG-100S dropped by 40 %, 26 %, and 29 %, respectively, when subjected to a sulfate solution for 60 days. The presence of 75 % GGBS results in the development of more compacts and an increase in the density of mixes, which decreases the void ratio and sulfate penetration due to the formation of extra geopolymerization products. This result is in agreement with the findings of earlier researchers (Garcia-Lodeiro et al., 2011; Deb et al., 2014; Elyamany et al., 2018). Moreover, the unreacted fine GGBS particles act as reinforcing agents. This fills the geopolymer matrix, enhances mechanical strength, and reduces porosity (Al-Majidi et al., 2016). Elyamany et al., (2018) studied the effect of binder type on geopolymer mortar $MgSO_4$ resistance. The findings revealed that FA mixes have the lowest residual compressive strength because they have the highest voids ratio compared to other geopolymer mixtures, allowing $MgSO_4$ solution to penetrate the pores of the specimen.

FTIR spectroscopy

The FTIR spectra in Fig. 15 show the changes in the chemical

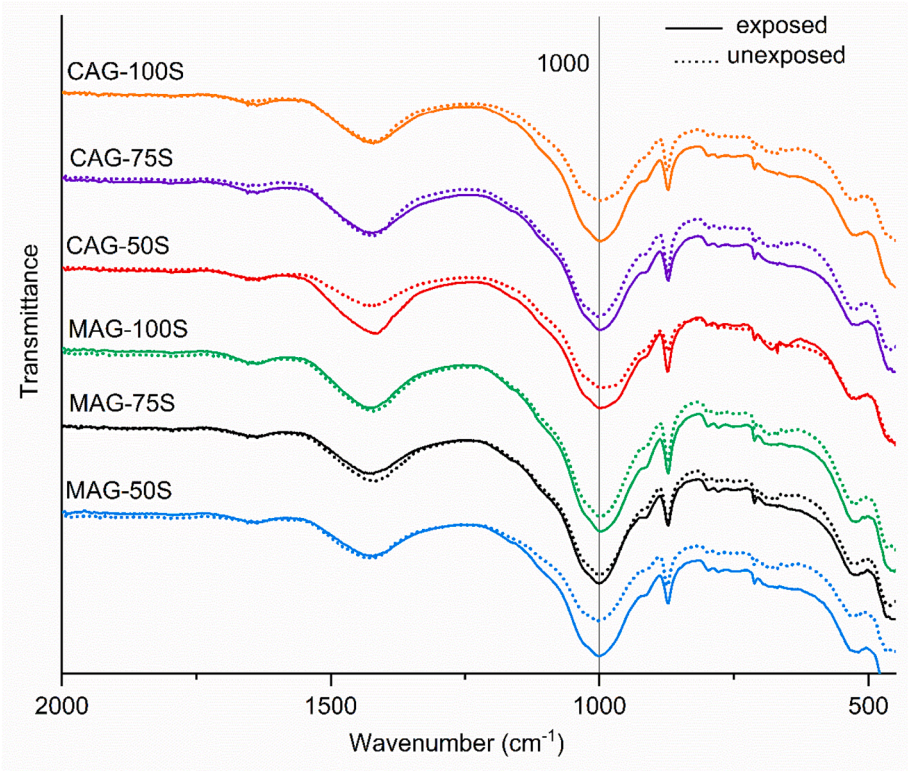

Fig. 15. FTIR spectra of MAG and CAG-stabilized soil control (unexposed) specimens compared to specimens exposed to $MgSO_4$ solutions for 120 days.

composition of the surface layer of DSM (MAG- and CAG) specimens when exposed to $MgSO_4$ solution. The spectra obtained from the inner sections of the specimens exposed to the sulfuric acid solution were compared to the spectra of the control specimens that were not exposed and were kept at ambient temperature. The control DSM specimens displayed a sharp peak at 1000 cm^{-1}, which is ascribed to asymmetric stretching of T-O bonds, where T can be either Al or Si. Additionally, a shoulder was observed at around 850–880 cm^{-1}, associated with M−O vibrations (K). The bending and stretching vibrations of water were identified by a broad peak centred at around 1425 cm^{-1} (Gao et al., 2013).

After exposing the DSM specimens to $MgSO_4$ solution, only minor changes were observed in the spectra. The only noticeable change was the increased intensity of the peak at 1000 cm^{-1} without any shift in its position. Findings akin to these were also described by (Kwasny et al., 2018). The increased intensity of the main band at 1000 cm^{-1} may be attributed to the magnesium sulfate attack raising the Si/Al ratio due to aluminium elimination from the binder (Burciaga-Díaz and Escalante-García, 2012). Bernal et al., (2012) found that the degree of a shift to higher wavenumbers in the infrared spectra of cement paste was related to the degree of structural damage to the binder, which was caused by exposure to acid attack. Specifically, as the degree of acid attack increased, the peak associated with the symmetric stretching of Si-O-Si shifted to higher wavenumbers, indicating a decrease in the Si-O-Si bond length due to the dissolution of the C-S-H gel. This shift was proportional to the degree of structural damage to the exposed samples. As seen in Fig. 15, MAG-75S samples exhibited no noticeable change in the spectra before and after exposure to the $MgSO_4$ attack environment, indicating that the MAG-75S samples maintained the original structure. Thus, the mechanochemical synthesis of geopolymer binder at 75 % GGBS substitution exhibited greater magnesium sulfate resistance.

Conclusions

In this study, a comparison was made between the mechanical and durability performance of the stabilized clayey soil with mechanochemically activated geopolymer and conventionally activated geopolymer. Geopolymer-stabilized soil samples were submerged in a 1 % magnesium sulfate solution. The effect of GGBS content on the long-term durability characteristics of geopolymer-stabilized soil was examined. The appearance, unconfined compressive strength (UCS), and mass changes of the samples were evaluated for their resistance to sulfate degradation.

- The UCS of the MAG-stabilized soil was 12–45 % higher than that of the CAG-stabilized soil. Moreover, the UCS of geopolymer-stabilized soil rose 114 %–361 % when GGBS content increased from 50 % to 100 %.
- The MAG-stabilized soil exhibits less mass change than the CAG-stabilized soil after 120 days of exposure to magnesium sulfate. This is attributed to mechanochemical activation, which increased the geopolymer binder's surface area and reactivity, leading to the filling of the pore system and inhibiting the penetration of magnesium sulfate. Furthermore, samples containing 100 % GGBS exhibited a lower mass change compared to those with 50 % and 75 % GGBS.
- The residual UCS of geopolymer stabilized soil decreased gradually with the increase of immersion age; the residual UCS for MAG-100S and CAG-100S specimens were 93 % and 89 % when exposed to 1 % magnesium sulfate solution for 60 days, whereas more declined to 70 % and 58 % respectively, after 120 days of immersion.
- The residual UCS of MAG-stabilized soil samples was 19–91 % larger than that of CAG-stabilized soil samples. In addition, the residual strength of geopolymer-stabilized soil specimens gradually increases as GGBS content increases. After 120 days, specimens containing 100 % FA had no residual UCS (fully damaged), whereas mixtures containing 100 % GGBS had a higher residual UCS.
- The FTIR spectra of MAG-100S and MAG-75S samples showed no significant changes after exposure to magnesium sulfate, indicating the maintenance of the original structure. It is revealed that the

mechanochemical synthesis of the geopolymer binder at 75 % and 100 % GGBS substitution demonstrated greater resistance to magnesium sulfate.

Funding

The authors declare that no funds, grants, or other support were received during the preparation of this manuscript.

CRediT authorship contribution statement

Mukhtar Hamid Abed: Conceptualization, Methodology, Data curation, Writing – original draft preparation, Investigation. **Firas Hamid Abed:** Methodology, Writing – original draft preparation, Investigation, Software. **Seyed Alireza Zareei:** Supervision. **Israa Sabbar Abbas:** Methodology, Writing – original draft preparation, Resources. **Hanifi Canakci:** Supervision. **Nahidh H. Kurdi:** Validation, Writing – review & editing. **Alireza Emami:** Supervision.

Declaration of competing interest

The authors declare that they have no known competing financial interests or personal relationships that could have appeared to influence the work reported in this paper.

Data availability

Data will be made available on request.

References

Abbas, I.S., Abed, M.H., Canakci, H., 2022. Development and characterization of eco-and user-friendly grout production via mechanochemical activation of geopolymer. J. Build. Eng., 105336

Abdullah, H.H., Shahin, M.A., Sarker, P., 2019. Use of Fly-Ash Geopolymer Incorporating Ground Granulated Slag for Stabilisation of Kaolin Clay Cured at Ambient Temperature. Geotech. Geol. Eng. 37, 721–740. https://doi.org/10.1007/s10706-018-0644-2.

Al-Majidi, M.H., Lampropoulos, A., Cundy, A., Meikle, S., 2016. Development of geopolymer mortar under ambient temperature for in situ applications. Constr. Build. Mater. 120, 198–211. https://doi.org/10.1016/j.conbuildmat.2016.05.085.

Anon, O.H., 1979. Classification of rocks and soils for engineering geological mapping. Part 1: rock and soil materials, Bull Int Assoc. Eng Geol. 19, 355–371.

Arulrajah, A., Yaghoubi, M., Disfani, M.M., Horpibulsuk, S., Bo, M.W., Leong, M., 2018. Evaluation of fly ash-and slag-based geopolymers for the improvement of a soft marine clay by deep soil mixing. Soils Found. 58, 1358–1370.

Astm, C., 2009. Standard test method for pulse velocity through concrete. ASTM Int, West Conshohocken, PA.

Baalamurugan, J., Ganesh Kumar, V., Stalin Dhas, T., Taran, S., Nalini, S., Karthick, V., Ravi, M., Govindaraju, K., 2021. Utilization of induction furnace steel slag based iron oxide nanocomposites for antibacterial studies, SN. Appl. Sci. 3, 1–8. https://doi.org/10.1007/s42452-021-04299-9.

Bakharev, T., 2005. Durability of geopolymer materials in sodium and magnesium sulfate solutions. Cem. Concr. Res. 35, 1233–1246. https://doi.org/10.1016/j.cemconres.2004.09.002.

Baláž, P., Achimovičová, M., Baláž, M., Billik, P., Cherkezova-Zheleva, Z., Criado, J.M., Delogu, F., Dutková, E., Gaffet, E., Gotor, F.J., 2013. others, Hallmarks of mechanochemistry: from nanoparticles to technology. Chem. Soc. Rev. 42, 7571–7637.

Bellato, D., Dalle Coste, A., Gerressen, F.W., Simonini, P., 2012. Long-term performance of CSM walls in slightly overconsolidated clays. ISSMGE-TC 211 Int. Symp. Gr. Improv. IS-GI.

Bernal, S.A., Rodr'iguez, E.D., de Gutiérrez, R., Provis, J.L., 2012. Performance of alkali-activated slag mortars exposed to acids. J. Sustain. Cem. Mater. 1, 138–151.

Bhadriraju, V., Puppala, A.J., Madhyannapu, R.S., Williammee, R., 2008. Laboratory procedure to obtain well-mixed soil binder samples of medium stiff to stiff expansive clayey soil for deep soil mixing simulation. Geotech. Test. J. 31, 225–238.

Bhardwaj, P., Gupta, R., Mishra, D., Sanghi, S.K., Verma, S., Amritphale, S.S., 2020. Corrosion and Fire Protective Behavior of Advanced Phosphatic Geopolymeric Coating on Mild Steel Substrate. Silicon. 12, 487–500. https://doi.org/10.1007/s12633-019-00153-1.

Bilondi, M.P., Toufigh, M.M., Toufigh, V., 2018. Experimental investigation of using a recycled glass powder-based geopolymer to improve the mechanical behavior of clay soils. Constr. Build. Mater. 170, 302–313.

Bonen, D., Cohen, M.D., 1992. Magnesium sulfate attack on portland cement paste—II. Chemical and mineralogical analyses. Cem. Concr. Res. 22, 707–718.

Bouazza, A., Kwan, P.S., Chapman, G., 2004. Strength properties of cement treated Coode Island Silt by the soil mixing method, in. Geotech. Eng. Transp. Proj. 1421–1428.

C. Bruce, J. Collin, R. Berg, G. Filz, M. Terashi, D. Yang, Federal Highway Administration Design Manual: Deep Mixing for Embankment and Foundation Support, October 2013 - FHWA-HRT-13-046, (2013) 244. http://www.fhwa.dot.gov/publications/research/infrastructure/structures/bridge/13046/index.cfm.

Burciaga-Díaz, O., Escalante-García, J.I., 2012. Strength and durability in acid media of alkali silicate-activated metakaolin geopolymers. J. Am. Ceram. Soc. 95, 2307–2313. https://doi.org/10.1111/j.1551-2916.2012.05249.x.

Çevik, A., Alzeebaree, R., Humur, G., Eren, M., 2018. E Ff Ect of Nano-Silica on the Chemical Durability and Mechanical Performance of Fl y Ash Based Geopolymer Concrete 44, 12253–12264. https://doi.org/10.1016/j.ceramint.2018.04.009.

Chew, S.H., Kamruzzaman, A.H.M., Lee, F.H., 2004. Physicochemical and Engineering Behavior of Cement Treated Clays. J. Geotech. Geoenvironmental Eng. 130, 696–706. https://doi.org/10.1061/(asce)1090-0241(2004)130:7(696).

D.P. Coduto, S.J. Abbey, S. Ngambi, B.E. Ngekpe, Geotechnical engineering: principles and practices, 1999.

Cyriaque Kaze, R., Naghizadeh, A., Tchadjie, L., Adesina, A., Noel Yankwa Djobo, J., Deutou Nemaleu, J.G., Kamseu, E., Chinje Melo, U., Tayeh, B.A., 2022. Lateritic soils based geopolymer materials: A review. Constr. Build. Mater. 344, 128157 https://doi.org/10.1016/j.conbuildmat.2022.128157.

Deb, P.S., Nath, P., Sarker, P.K., 2014. The effects of ground granulated blast-furnace slag blending with fly ash and activator content on the workability and strength properties of geopolymer concrete cured at ambient temperature. Mater. Des. 62, 32–39. https://doi.org/10.1016/j.matdes.2014.05.001.

N. Denies, N. Huybrechts, F. De Cock, B. Lameire, J. Maertens, A. Vervoort, A. Guimond-Barrett, Thoughts on the durability of the soil mix material, in: 2015.

Duxson, P., Provis, J.L., 2008. Designing precursors for geopolymer cements. J. Am. Ceram. Soc. 91, 3864–3869. https://doi.org/10.1111/j.1551-2916.2008.02787.x.

Elyamany, H.E., Abd Elmoaty, M., Elshaboury, A.M., 2018. Magnesium sulfate resistance of geopolymer mortar. Constr. Build. Mater. 184, 111–127.

Elyamany, H.E., Abd Elmoaty, A.E.M., Elshaboury, A.M., Abd Elmoaty, M., Elshaboury, A.M., 2018. Magnesium sulfate resistance of geopolymer mortar. Constr. Build. Mater. 184, 111–127. https://doi.org/10.1016/j.conbuildmat.2018.06.212.

Favier, A., Hot, J., Habert, G., Roussel, N., D'Espinose De Lacaillerie, J.B., 2014. Flow properties of MK-based geopolymer pastes. A Comparative Study with Standard Portland Cement Pastes, Soft Matter. 10, 1134–1141. https://doi.org/10.1039/c3sm51889b.

Gao, X.X., Michaud, P., Joussein, E., Rossignol, S., 2013. Behavior of metakaolin-based potassium geopolymers in acidic solutions. J. Non. Cryst. Solids. 380, 95–102. https://doi.org/10.1016/j.jnoncrysol.2013.09.002.

Garcia-Lodeiro, I., Palomo, A., Fernández-Jiménez, A., MacPhee, D.E., 2011. Compatibility studies between N-A-S-H and C-A-S-H gels. Study in the ternary diagram Na2O-CaO-Al2O3-SiO 2–H2O. Cem. Concr. Res. 41, 923–931. https://doi.org/10.1016/j.cemconres.2011.05.006.

Goncalves, J., El-Bakkari, M., Boluk, Y., Bindiganavile, V., 2019. Cellulose nanofibres (CNF) for sulphate resistance in cement based systems. Cem. Concr. Compos. 99, 100–111. https://doi.org/10.1016/j.cemconcomp.2019.03.005.

Gopalakrishnan, R., Chinnaraju, K., 2019. Durability of ambient cured alumina silicate concrete based on slag/fly ash blends against sulfate environment. Constr. Build. Mater. 204, 70–83. https://doi.org/10.1016/j.conbuildmat.2019.01.153.

Güllü, H., Ali Agha, A., 2021. The rheological, fresh and strength effects of cold-bonded geopolymer made with metakaolin and slag for grouting. Constr. Build. Mater. 274, 122091 https://doi.org/10.1016/j.conbuildmat.2020.122091.

Güllü, H., Canakci, H., Al Zangana, I.F., 2017. Use of cement based grout with glass powder for deep mixing. Constr. Build. Mater. 137, 12–20.

Gupta, R., Bhardwaj, P., Mishra, D., Prasad, M., Amritphale, S.S., 2017. Formulation of mechanochemically evolved fly ash based hybrid inorganic–organic geopolymers with multilevel characterization. J. Inorg. Organomet. Polym. Mater. 27, 385–398. https://doi.org/10.1007/s10904-016-0461-0.

Gupta, R., Bhardwaj, P., Mishra, D., Mudgal, M., Chouhan, R.K., Prasad, M., Amritphale, S.S., 2017. Evolution of advanced geopolymeric cementitious material via a novel process. Adv. Cem. Res. 29, 125–134. https://doi.org/10.1680/jadcr.16.00113.

Gupta, R., Tomar, A.S., Mishra, D., Sanghi, S.K., 2020. Multinuclear MAS NMR Characterization of Fly-Ash-Based Advanced Sodium Aluminosilicate Geopolymer: Exploring Solid-State Reactions. ChemistrySelect. 5, 4920–4927. https://doi.org/10.1002/slct.202000203.

Hamid Abed, M., Abbas, I.S., Canakci, H., 2022a. Effect of glass powder on the rheological and mechanical properties of slag-based mechanochemical activation geopolymer grout. Eur. J. Environ. Civ. Eng. 1–25. https://doi.org/10.1080/19648189.2022.2145374.

Hamid Abed, M., Abbas, I.S., Canakci, H., 2022c. Influence of mechanochemical activation on the rheological, fresh, and mechanical properties of one-part geopolymer grout. Adv. Cem. Res. 1–38.

Hamid Abed, M., Sabbar Abbas, I., Hamed, M., Canakci, H., 2022b. Rheological, fresh, and mechanical properties of mechanochemically activated geopolymer grout: A comparative study with conventionally activated geopolymer grout. Constr. Build. Mater. 322, 126338 https://doi.org/10.1016/j.conbuildmat.2022.126338.

Helson, O., Eslami, J., Beaucour, A.L., Noumowe, A., Gotteland, P., 2018. Durability of soil mix material subjected to wetting/drying cycles and external sulfate attacks. Constr. Build. Mater. 192, 416–428. https://doi.org/10.1016/j.conbuildmat.2018.10.095.

Horpibulsuk, S., Rachan, R., Suddeepong, A., 2011. Assessment of strength development in blended cement admixed Bangkok clay. Constr. Build. Mater. 25, 1521–1531. https://doi.org/10.1016/j.conbuildmat.2010.08.006.
Hosseini, S., Brake, N.A., Nikookar, M., Günaydın-Şen, Ö., Snyder, H.A., 2021. Mechanochemically activated bottom ash-fly ash geopolymer. Cem. Concr. Compos. 118 https://doi.org/10.1016/j.cemconcomp.2021.103976.
Ikegami, M., Ichiba, T., Ohishi, K., Terashi, M., 2003. Long-term strength change of cement treated soil at Daikoku Pier. In: Soft Gr. Eng. Coast. Areas, AA Balkema the Netherlands, pp. 241–246.
Indu Siva Ranjani, G., Ramamurthy, K., 2012. Behaviour of foam concrete under sulphate environments. Cem. Concr. Compos. 34, 825–834. https://doi.org/10.1016/j.cemconcomp.2012.03.007.
Intini, G., Liberti, L., Notarnicola, M., Di Canio, F., 2009. Mechanochemical activation of coal fly ash for production of high strength cement conglomerates. ХиМия в Интересах Устойчивого Развития. 17, 567–571.
Jiang, N.J., Du, Y.J., Liu, K., 2018. Durability of lightweight alkali-activated ground granulated blast furnace slag (GGBS) stabilized clayey soils subjected to sulfate attack. Appl. Clay Sci. 161, 70–75. https://doi.org/10.1016/j.clay.2018.04.014.
Juenger, M.C.G., Winnefeld, F., Provis, J.L., Ideker, J.H., 2011. Advances in alternative cementitious binders. Cem. Concr. Res. 41, 1232–1243. https://doi.org/10.1016/j.cemconres.2010.11.012.
Kamon, M., Nontananandh, S., Katsumi, T., 1993. Utilization of stainless-steel slag by cement hardening. Soils Found. 33, 118–129. https://doi.org/10.3208/sandf1972.33.3_118.
Kaze, C.R., Lecomte-Nana, G.L., Kamseu, E., Camacho, P.S., Yorkshire, A.S., Provis, J.L., Duttine, M., Wattiaux, A., Melo, U.C., 2021. Mechanical and physical properties of inorganic polymer cement made of iron-rich laterite and lateritic clay: A comparative study. Cem. Concr. Res. 140 https://doi.org/10.1016/j.cemconres.2020.106320.
Kumar, S., Kumar, R., 2011. Mechanical activation of fly ash: Effect on reaction, structure and properties of resulting geopolymer. Ceram. Int. 37, 533–541.
Kumar, S., Kumar, R., Mehrotra, S.P., 2010. Influence of granulated blast furnace slag on the reaction, structure and properties of fly ash based geopolymer. J. Mater. Sci. 45, 607–615. https://doi.org/10.1007/s10853-009-3934-5.
Kushwah, S., Mudgal, M., Chouhan, R.K., 2021. The Process, Characterization and Mechanical properties of fly ash-based Solid form geopolymer via mechanical activation, South African. J Chem. Eng. 38, 104–114. https://doi.org/10.1016/j.sajce.2021.09.002.
Kwasny, J., Aiken, T.A., Soutsos, M.N., McIntosh, J.A., Cleland, D.J., 2018. Sulfate and acid resistance of lithomarge-based geopolymer mortars. Constr. Build. Mater. 166, 537–553. https://doi.org/10.1016/j.conbuildmat.2018.01.129.
Lee, N.K., Lee, H.K., 2013. Setting and mechanical properties of alkali-activated fly ash/slag concrete manufactured at room temperature. Constr. Build. Mater. 47, 1201–1209. https://doi.org/10.1016/j.conbuildmat.2013.05.107.
Lee, W.K.W., Van Deventer, J.S.J., 2003. Use of Infrared Spectroscopy to Study Geopolymerization of Heterogeneous Amorphous Aluminosilicates. Langmuir. 19, 8726–8734. https://doi.org/10.1021/la026127e.
W.K.W. Lee, J.S. J, Structural reorganisation of class F fly ash in alkaline silicate solutions, 211 (2002) 49–66.
Luo, Z., Zhang, B., Zou, J., Luo, B., 2022. Case Studies in Construction Materials Sulfate erosion resistance of slag-fly ash based geopolymer stabilized soft soil under semi-immersion condition. Case Stud. Constr. Mater. 17, e01506.
M. Manish, C.R. Kumar, M. Deepti, F. Application, P. Data, (12) United States Patent, 2 (2016).
Matalkah, F., Xu, L., Wu, W., Soroushian, P., 2017. Mechanochemical synthesis of one-part alkali aluminosilicate hydraulic cement. Mater. Struct. 50, 1–12. https://doi.org/10.1617/s11527-016-0968-4.
Mudgal, M., Chouhan, R.K., Kushwah, S., Srivastava, A.K., 2019. Enhancing reactivity and properties of fly-ash-based solid-form geopolymer via ball-milling, Emerg. Mater. Res. 9, 2–9.
Nath, S.K., Kumar, S., 2013. Influence of iron making slags on strength and microstructure of fly ash geopolymer. Constr. Build. Mater. 38, 924–930. https://doi.org/10.1016/j.conbuildmat.2012.09.070.
Nath, S.K., Kumar, S., 2019. Influence of Granulated Silico-Manganese Slag on Compressive Strength and Microstructure of Ambient Cured Alkali-Activated Fly Ash Binder. Waste and Biomass Valorization. 10, 2045–2055. https://doi.org/10.1007/s12649-018-0213-1.
Nedunuri, A.S.S.S., Muhammad, S., 2020. Influential parameters in rheology of alkali-activated binders. ACI Mater. J. 117, 75–85. https://doi.org/10.14359/51724593.
Nochaiya, T., Wongkeo, W., Pimraksa, K., Chaipanich, A., 2010. Microstructural, physical, and thermal analyses of Portland cement-fly ash-calcium hydroxide blended pastes. J. Therm. Anal. Calorim. 100, 101–108. https://doi.org/10.1007/s10973-009-0491-8.
Pacheco-Torgal, F., Castro-Gomes, J., Jalali, S., 2008. Alkali-activated binders: A review. Part 2. About materials and binders manufacture. Constr. Build. Mater. 22, 1315–1322.
Pacheco-Torgal, F., Moura, D., Ding, Y., Jalali, S., 2011. Composition, strength and workability of alkali-activated metakaolin based mortars. Constr. Build. Mater. 25, 3732–3745.
Pakbaz, M.S., Farzi, M., 2015. Comparison of the effect of mixing methods (dry vs. wet) on mechanical and hydraulic properties of treated soil with cement or lime. Appl. Clay Sci. 105, 156–169.
Palacios, M., Banfill, P.F.G., Puertas, F., 2008. Rheology and setting of alkali-activated slag pastes and mortars: Effect of organic admixture. ACI Mater. J. 105, 140.
Phummiphan, I., Horpibulsuk, S., Sukmak, P., Chinkulkijniwat, A., Arulrajah, A., Shen, S. L., 2016. Stabilisation of marginal lateritic soil using high calcium fly ash-based geopolymer. Road Mater. Pavement Des. 17, 877–891. https://doi.org/10.1080/14680629.2015.1132632.
Porbaha, A., 1998. State of the art in deep mixing technology: part I. Basic concepts and overview. Proc. Inst. Civ. Eng. Improv. 2, 81–92.
Puppala, A.J., Wattanasanticharoen, E., Dronamraju, V.S., Hoyos, L.R., 2007. Ettringite induced heaving and shrinking in kaolinite clay. Probl. Soils Rocks Situ Charact. 1–10.
Rios, S., Ramos, C., Viana da Fonseca, A., Cruz, N., Rodrigues, C., 2019. Mechanical and durability properties of a soil stabilised with an alkali-activated cement. Eur. J. Environ. Civ. Eng. 23, 245–267. https://doi.org/10.1080/19648189.2016.1275987.
Ryu, G.S., Lee, Y.B., Koh, K.T., Chung, Y.S., 2013. The mechanical properties of fly ash-based geopolymer concrete with alkaline activators. Constr. Build. Mater. 47, 409–418. https://doi.org/10.1016/j.conbuildmat.2013.05.069.
Salami, B.A., Megat Johari, M.A., Ahmad, Z.A., Maslehuddin, M., 2017. Durability performance of Palm Oil Fuel Ash-based Engineered Alkaline-activated Cementitious Composite (POFA-EACC) mortar in sulfate environment. Constr. Build. Mater. 131, 229–244. https://doi.org/10.1016/j.conbuildmat.2016.11.048.
Sargent, P., Hughes, P.N., Rouainia, M., 2016. A new low carbon cementitious binder for stabilising weak ground conditions through deep soil mixing. Soils Found. 56, 1021–1034. https://doi.org/10.1016/j.sandf.2016.11.007.
Shen, S.L., Huang, X.C., Du, S.J., Han, J., 2003. Laboratory studies on property changes in surrounding clays due to installation of deep mixing columns. Mar. Georesources Geotechnol. 21, 15–35. https://doi.org/10.1080/10641190306711.
Sherwood, P.T., 1962. Effect of sulfates on cement-and lime-stabilized soils. Highw. Res, Board Bull.
Souri, A., Kazemi-Kamyab, H., Snellings, R., Naghizadeh, R., Golestani-Fard, F., Scrivener, K., 2015. Pozzolanic activity of mechanochemically and thermally activated kaolins in cement. Cem. Concr. Res. 77, 47–59.
Teerawattanasuk, C., Voottipruex, P., 2019. Comparison between cement and fly ash geopolymer for stabilized marginal lateritic soil as road material. Int. J. Pavement Eng. 20, 1264–1274. https://doi.org/10.1080/10298436.2017.1402593.
Thokchom, S., Ghosh, P., Ghosh, S., 2010. Performance of fly ash based geopolymer mortars in sulphate solution. J. Eng. Sci. Technol. Rev. 3, 36–40. https://doi.org/10.25103/jestr.031.07.
Tian, B., Cohen, M.D., 2000. Does gypsum formation during sulfate attack on concrete lead to expansion? Cem. Concr. Res. 30, 117–123. https://doi.org/10.1016/S0008-8846(99)00211-2.
Verástegui-Flores, R.D., Di Emidio, G., 2014. Impact of sulfate attack on mechanical properties and hydraulic conductivity of a cement-admixed clay. Appl. Clay Sci. 101, 490–496. https://doi.org/10.1016/j.clay.2014.09.012.
Yaghoubi, M., Arulrajah, A., Disfani, M.M., Horpibulsuk, S., Darmawan, S., Wang, J., 2019. Impact of field conditions on the strength development of a geopolymer stabilized marine clay. Appl. Clay Sci. 167, 33–42. https://doi.org/10.1016/j.clay.2018.10.005.
Ye, H., Chen, Z., Huang, L., 2019. Mechanism of sulfate attack on alkali-activated slag: The role of activator composition. Cem. Concr. Res. 125, 105868 https://doi.org/10.1016/j.cemconres.2019.105868.
Yusuf, M.O., Johari, M.A.M., Ahmad, Z.A., Maslehuddin, M., 2014. Effects of addition of Al(OH)3 on the strength of alkaline activated ground blast furnace slag-ultrafine palm oil fuel ash (AAGU) based binder. Constr. Build. Mater. 50, 361–367. https://doi.org/10.1016/j.conbuildmat.2013.09.054.
Zhang, M., Guo, H., El-Korchi, T., Zhang, G., Tao, M., 2013. Experimental feasibility study of geopolymer as the next-generation soil stabilizer. Constr. Build. Mater. 47, 1468–1478.
Zhang, Y.J., Zhao, Y.L., Li, H.H., Xu, D.L., 2008. Structure characterization of hydration products generated by alkaline activation of granulated blast furnace slag. J. Mater. Sci. 43, 7141–7147. https://doi.org/10.1007/s10853-008-3028-9.
Zhao, F.Q., Ni, W., Wang, H.J., Liu, H.J., 2007. Activated fly ash/slag blended cement. Resour. Conserv. Recycl. 52, 303–313. https://doi.org/10.1016/j.resconrec.2007.04.002.
Zhu, H., Liang, G., Li, H., Wu, Q., Zhang, C., Yin, Z., Hua, S., 2021. Insights to the sulfate resistance and microstructures of alkali-activated metakaolin/slag pastes. Appl. Clay Sci. 202, 105968 https://doi.org/10.1016/j.clay.2020.105968.
Zhuang, X.Y., Chen, L., Komarneni, S., Zhou, C.H., Tong, D.S., Yang, H.M., Yu, W.H., Wang, H., 2016. Fly ash-based geopolymer: Clean production, properties and applications. J. Clean. Prod. 125, 253–267. https://doi.org/10.1016/j.jclepro.2016.03.019.